

ESC and KAIT observations of the transitional Type Ia SN 2004eo

A. Pastorello,^{1,2*} P. A. Mazzali,^{1,3} G. Pignata,⁴ S. Benetti,⁵ E. Cappellaro,⁵
 A. V. Filippenko,⁶ W. Li,⁶ W. P. S. Meikle,⁷ A. A. Arkharov,⁸ G. Blanc,^{5,9}
 F. Bufano,^{5,10} A. Derekas,¹¹ M. Dolci,¹² N. Elias-Rosa,^{1,5,13} R. J. Foley,⁶
 M. Ganeshalingam,⁶ A. Harutyunyan,^{5,10} L. L. Kiss,¹¹ R. Kotak,^{2,7,14}
 V. M. Larionov,^{8,15} J. R. Lucey,¹⁶ N. Napoleone,¹⁷ H. Navasardyan,⁵ F. Patat,¹⁴
 J. Rich,¹⁸ S. D. Ryder,¹⁹ M. Salvo,¹⁸ B. P. Schmidt,¹⁸ V. Stanishev,²⁰ P. Székely,²¹
 S. Taubenberger,¹ S. Temporin,^{22,23} M. Turatto⁵ and W. Hillebrandt¹

¹Max-Planck-Institut für Astrophysik, Karl-Schwarzschild-Str. 1, 85741 Garching bei München, Germany

²Astrophysics Research Centre, School of Mathematics and Physics, Queen's University Belfast, Belfast BT7 1NN

³INAF Osservatorio Astronomico di Trieste, Via Tiepolo 11, 34131 Trieste, Italy

⁴Pontificia Universidad Católica de Chile, Departamento de Astronomía y Astrofísica, Campus San Joaquín, Vicuña Mackenna 4860, Casilla 306, Santiago 22, Chile

⁵INAF Osservatorio Astronomico di Padova, Vicolo dell'Osservatorio 5, 35122 Padova, Italy

⁶Department of Astronomy, University of California, Berkeley, CA 94720-3411, USA

⁷Astrophysics Group, Imperial College London, Blackett Laboratory, Prince Consort Road, London SW7 2AZ

⁸Central Astronomical Observatory of Pulkovo, 196140 St Petersburg, Russia

⁹APC, UMR 7164 (CNRS, Université Paris 7, CEA, Observatoire de Paris), 10, rue Alice Domon et Lie Duquet, F-75205 Paris Cedex 13, France

¹⁰Dipartimento di Astronomia, Università di Padova, Vicolo dell'Osservatorio, 2, I-35122 Padova, Italy

¹¹School of Physics A28, University of Sydney, NSW 2006, Australia

¹²INAF Osservatorio Astronomico di Collurania, via M. Maggini, 64100 Teramo, Italy

¹³Universidad de La Laguna, Av. Astrofísico Francisco Sánchez s/n, E-38206 La Laguna, Tenerife, Spain

¹⁴European Southern Observatory (ESO), Karl-Schwarzschild-Str. 2, 85748, Garching bei München, Germany

¹⁵Astronomical Institute of St Petersburg University, St Petersburg, Petrodvorets, Universitetsky pr. 28, 198504 St Petersburg, Russia

¹⁶Department of Physics, University of Durham, South Road, Durham DH1 3LE

¹⁷INAF Osservatorio Astronomico di Roma, Via di Frascati 33, I-00040 Monte Porzio Catone, Italy

¹⁸Research School of Astronomy and Astrophysics, Australian National University, Mount Stromlo and Siding Spring Observatories Cotter Road, Weston Creek, ACT 2611, Australia

¹⁹Anglo-Australian Observatory, PO Box 296, Epping, NSW 1710, Australia

²⁰Department of Physics, Stockholm University, AlbaNova University Centre, SE-10691 Stockholm, Sweden

²¹Department of Experimental Physics & Astronomical Observatory, University of Szeged, H-6720 Szeged, Dóm tér 9, Hungary

²²Institut für Astro- und Teilchenphysik, Leopold-Franzens-Universität Innsbruck, Technikerstr. 25, A-6020 Innsbruck, Austria

²³CEA/DSM/DAPNIA, Service d'Astrophysique, Saclay, F-91191 Gif-sur-Yvette Cedex, France

Accepted 2007 March 6. Received 2007 March 5; in original form 2007 February 15

ABSTRACT

We present optical and infrared observations of the unusual Type Ia supernova (SN) 2004eo. The light curves and spectra closely resemble those of the prototypical SN 1992A, and the luminosity at maximum ($M_B = -19.08$) is close to the average for a Type Ia supernova (SN Ia). However, the ejected ^{56}Ni mass derived by modelling the bolometric light curve (about $0.45 M_\odot$) lies near the lower limit of the ^{56}Ni mass distribution observed in normal SNe Ia. Accordingly, SN 2004eo shows a relatively rapid post-maximum decline in the light curve [$\Delta m_{15}(B)_{\text{true}} = 1.46$], small expansion velocities in the ejecta and a depth ratio $\text{Si II } \lambda 5972/\text{Si II } \lambda 6355$ similar to that of SN 1992A. The physical properties of SN 2004eo cause it to fall very close to the boundary between the faint, low-velocity gradient and high-velocity gradient subgroups proposed by Benetti et al. Similar behaviour is seen in a

*E-mail: pasto@MPA-Garching.MPG.DE

few other SNe Ia. Thus, there may in fact exist a few SNe Ia with intermediate physical properties.

Key words: supernovae: general – supernovae: individual: SN 2004eo – supernovae: individual: SN 1992A – galaxies: individual: NGC 6928.

1 INTRODUCTION

Thermonuclear supernovae (SNe) are among the most important cosmological distance indicators (see Filippenko 2005 for a recent review). Consequently, over the course of the last few years, much effort has been made to obtain extensive data sets. The modelling of such high-quality data, particularly in three dimensions, should help improve our understanding of the thermonuclear explosion mechanisms.

This work adds to the data base of observations of nearby Type Ia supernovae (SNe Ia), obtained by the European Supernova Collaboration (ESC)¹ as part of a European Research Training Network (RTN). The first supernova targeted by the collaboration was SN 2002bo (Benetti et al. 2004). Since then, 15 other nearby SNe Ia (see Pastorello et al. 2007 and references therein) and one peculiar SN Ic (SN 2004aw, initially misclassified as a SN Ia; Taubenberger et al. 2006) have been monitored by the ESC. In addition, three papers based on ESC data and discussing systematic properties of SNe Ia have been published. Benetti et al. (2005) found evidence that thermonuclear SNe cluster in three different subgroups on the basis of the observed spectrophotometric properties [faint, low-velocity gradient (LVG) and high-velocity gradient (HVG) SNe Ia]. In an effort to find clues to explain this diversity, Hachinger, Mazzali & Benetti (2006) explored the behaviour of a number of other spectroscopic parameters of SNe Ia. They found that the equivalent width ratios of some spectral lines (mainly Si II λ 5972 and λ 6355, S II and Fe II) correlate with $\Delta m_{15}(B)$ (as defined by Phillips 1993). Also, using the spectra of a number of SNe followed by the ESC, Mazzali et al. (2005) showed that high-velocity features, whose existence was first proposed by Hatano et al. (1999) in early-time spectra of SN 1994D, are actually a common characteristic of SNe Ia.

The discovery of SN 2004eo provided an ideal opportunity for increasing the sample of well-monitored, apparently normal SNe Ia. It fulfilled the selection criteria specified by the ESC – it was a relatively nearby ($v_{\text{rec}} < 6000 \text{ km s}^{-1}$) SN discovered well before maximum light. Moreover, because of its proximity to the celestial equator, SN 2004eo was observable from both hemispheres, allowing us to exploit all telescopes accessible to the various nodes of the collaboration. Finally, the location of SN 2004eo at the outskirts of its host galaxy allowed for accurate photometric measurements and suggested minimal internal extinction.

In this paper, we present the spectroscopic and photometric observations of SN 2004eo, ranging from 11 d before maximum light to more than 1 yr after maximum. Most of the data have been collected by the ESC, with additional contributions (generally photometry) from the SN groups of the University of California (Berkeley) and of the Osservatorio Astronomico di Collurania (Italy).

This paper is organized as follows. In Section 2, we describe the observations, including instrument details and data reduction

techniques. In Section 3, we show the optical and infrared (IR) light curves of SN 2004eo, present the colour evolution and bolometric light curve, and analyse the parameters derived from the photometry. Section 4 is devoted to the study of the optical and IR spectroscopic evolution of SN 2004eo. A discussion and a short summary follow in Sections 5 and 6, respectively.

2 OBSERVATIONS

2.1 SN 2004eo and NGC 6928

SN 2004eo was discovered by K. Itagaki (Arbour et al. 2004) on 2004 September 17.5 (UT dates are used throughout this paper) at a magnitude of 17.8. The SN coordinates are $\alpha = 20^{\text{h}}32^{\text{m}}54^{\text{s}}.19$, $\delta = +09^{\circ}55'42''.7$. It lies 59.1 arcsec E and 6.5 arcsec N of the nucleus of the host galaxy, NGC 6928 (cf. Table 1). The location of the SN (Fig. 1) suggests small host-galaxy extinction. This is supported by spectroscopic evidence (see Section 4).

The SN 2004eo early-time spectrum is dominated by Si II and S II lines, showing that the SN was a Type Ia event (Gonzalez et al. 2004). The relatively high velocities in the classification spectrum indicate that the SN was discovered soon after explosion. Indeed, the SN was not detected on September 12 (limiting magnitude 18.5), only a few days before discovery (Arbour et al. 2004). This, together with subsequent observations, means that the light curve of SN 2004eo is one of the most complete of any known SN.

2.2 ESC and KAIT observations

SN 2004eo was monitored extensively, especially in B , V , R and I photometry and optical spectroscopy. Observations cover a period from about 11 d before B -band maximum to about three months after maximum. Henceforth, we adopt as reference the epoch of the B -band maximum (see below). The U and IR bands were less densely sampled, with the observations only starting after maximum light. Due to the seasonal gap, the SN was not observed for three months, between about 100 and 190 d past maximum. In view of the slow evolution at late (nebular) phases, subsequent observations were less frequent than near maximum. On day +228, a high-quality nebular spectrum of SN 2004eo was obtained with the VLT. The log of all optical and IR spectra is given in Table 2. The photometric data are presented in Section 3.

During the optical monitoring of SN 2004eo, 12 different instruments were employed. The instruments are as follows:

(i) 2.3-m telescope of the Siding Spring Observatory (Australia), MSSSO11 imager (0.59 arcsec pixel⁻¹); for spectroscopy the Double Beam Spectrograph was used (2048 × 512 pixel E2V CCD4210 detector in the blue arm; Site 1752 × 532 pixel detector in the red arm).

(ii) 0.76-m Katzman Automatic Imaging Telescope (KAIT; Filippenko et al. 2001) of the Lick Observatory (Mt Hamilton, California, USA) (SITE AP7 CCD, 0.8 arcsec pixel⁻¹);

¹ <http://www.mpa-garching.mpg.de/~rtn>

Table 1. Main parameters of NGC 6928 and SN 2004eo.

NGC 6928		
Galaxy type	SB(s)ab	1
α (J2000.0)	20 ^h 32 ^m 50 ^s .22	1
δ (J2000.0)	+09°55′35″.1	1
B_{tot}	13.40	2
Diameter	2.0 × 0.6 arcmin ²	1
v_{rad}	4707 km s ⁻¹	3
v_{vir}	4809 km s ⁻¹	2
μ^a	34.12 ± 0.10	2
SN 2004eo		
α (J2000.0)	20 ^h 32 ^m 54 ^s .19	5
δ (J2000.0)	+09°55′42″.7	5
Offset SN Galaxy	59.1 arcsec E, 6.5 arcsec N	5
SN Type	Ia	6
$E(B - V)_{\text{host}}$	0	7
$E(B - V)_{\text{Gal}}$	0.109	4
Discovery date (UT)	2004 Sep. 17.5	5
Discovery mag.	17.8	5
Predisc. limit date (UT)	2004 Sep. 12	5
Limit mag.	18.5	5
B_{max} epoch (UT)	2004 Sep. 30.7	7
B_{max} epoch (JD)	245 3279.2	7
B_{max}	15.51	7
$M_{B,\text{max}}$	-19.08	7
$\Delta m_{15}(B)_{\text{obs}}$	1.45	7
$\Delta m_{15}(B)_{\text{true}}$	1.46	7
s^{-1}	1.12	7
ΔC_{12}	0.49	7
t_r	17.7	7
$M_{\text{Ni}} (M_{\odot})$	0.45	7

^aComputed with $H_0 = 72 \text{ km s}^{-1} \text{ Mpc}^{-1}$.

1 = NED (available at <http://nedwww.ipac.caltech.edu>); 2 = LEDA (available at <http://leda.univ-lyon1.fr>); 3 = Theureau et al. (1998); 4 = Schlegel et al. (1998); 5 = Arbour et al. (2004); 6 = Gonzalez et al. (2004) and 7 = this paper.

(iii) Liverpool Telescope (La Palma, Canary Islands, Spain), RATCAM (optical CCD, 0.27 arcsec pixel⁻¹);

(iv) Nordic Optical Telescope (La Palma), ALFOSC (E2V 2048 × 2048 pixel CCD42-40 detector, 0.19 arcsec pixel⁻¹);

(v) 1-m telescope of the Siding Spring Observatory (Australia), Wide Field Camera (eight 2048 × 4096 pixel CCDs, 0.375 arcsec pixel⁻¹);

(vi) Calar Alto 2.2-m telescope (Spain), CAFOS (Site CCD, 0.53 arcsec pixel⁻¹);

(vii) Tenagra II 0.81-m telescope (Arizona, US) (Site CCD, 0.87 arcsec pixel⁻¹);

(viii) Copernico 1.82-m telescope of Mt Ekar (Asiago, Italy), AFOSC (TEK 1024 × 1024 pixel thinned CCD, 0.473 arcsec pixel⁻¹);

(ix) ESO/MPI 2.2-m telescope (La Silla, Chile), Wide Field Imager (mosaic of eight 2048 × 4096 pixel CCDs, 0.24 arcsec pixel⁻¹);

(x) VLT-Antu telescope (Cerro Paranal, Chile), FORS1 (2048 × 2046 pixel CCD detector, 0.2 arcsec pixel⁻¹);

(xi) Telescopio Nazionale Galileo (TNG) (La Palma), DOLORES (2048 × 4096 pixel Loral CCD, 0.275 arcsec pixel⁻¹);

(xii) William Herschel Telescope (WHT) (La Palma), ISIS (2048 × 4096 pixel EEV12 CCD, 0.19 arcsec pixel⁻¹ in the blue arm; 2047 × 4611 pixel Marconi2 CCD, 0.20 arcsec pixel⁻¹ in the red arm); and

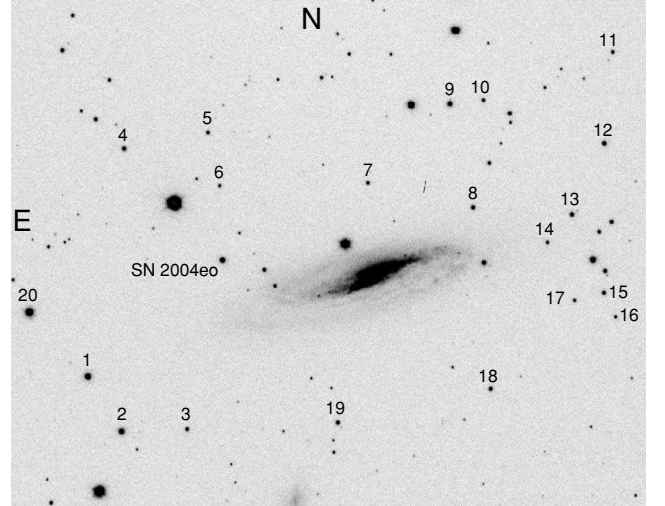


Figure 1. SN 2004eo and a local sequence of stars in the field of NGC 6928. (V-band image, obtained on 2004 October 2 with the Northern Optical Telescope equipped with ALFOSC.)

(xiii) Shane 3-m telescope (Lick Observatory), Kast Double Spectrograph [two UV-flooded Reticon 1200 × 400 pixel devices (one per arm), 0.8 arcsec pixel⁻¹].

In addition, six different instrumental configurations were used to collect the IR data as follows.

(i) AZT-24 1.08-m telescope of Campo Imperatore (Italy) SWIRCAM (1.04 arcsec pixel⁻¹);

(ii) 3.58-m TNG (La Palma), NICS (HgCdTe Hawaii 1024 × 1024 pixel array, 0.25 arcsec pixel⁻¹);

(iii) Anglo-Australian Telescope (AAT) of the Siding Spring Observatory, IRIS2 (1024 × 1024 pixel HgCd Te array, 0.45 arcsec pixel⁻¹);

(iv) WHT (La Palma), LIRIS (Hawaii 1024 × 1024 pixel HgCdTe array, 0.25 arcsec pixel⁻¹);

(v) Calar Alto 3.5-m telescope, Omega2000 (2048 × 2048 pixel HAWAII-2 CCD, 0.45 arcsec pixel⁻¹) and

(vi) the VLT-Antu module, ISAAC (1024 × 1024 pixel InSb Aladdin array, 0.148 arcsec pixel⁻¹).

The use of a large number of different instruments required careful homogenization of our data set. This is discussed in Section 3.

2.3 Data reduction

All optical photometric images were pre-reduced (i.e. overscan, bias, flat-field corrected and trimmed) using standard IRAF² procedures. Because of the high brightness of the night sky in the IR, both imaging and spectroscopy required some additional data processing, including the creation of clean sky images and their subtraction from the target frames. Finally, the resulting images were spatially registered and combined in order to improve the signal-to-noise ratio (S/N).

² IRAF is distributed by the National Optical Astronomy Observatories, which are operated by the Association of Universities for Research in Astronomy, Inc. under contract with the National Science Foundation.

Table 2. Optical and IR spectroscopic observations of SN 2004eo.

Date	JD 2400000	Phase ^a (d)	Instrumental configuration	Grism or grating	Resolution (Å)	Exp. time (s)	Range (Å)	Standard star
19/09/04	53268.05	-11.3	SSO2.3m+DBS	B+R	4.8,4.8	1200(x2)+1200(x2)	3500–9200	Feige110
24/09/04	53272.74	-6.6	Lick-Shane 3-m+Kast	<i>b</i>	6.2,9.6	1000+1000	3340–10700	BD+284211,BD+174708
27/09/04	53276.39	-2.9	WHT+ISIS	R300B+R158R	3.6,6.5	900(x2)+900(x2)	3070–10670	BD+284211
02/10/04	53281.45	+2.2	NOT+ALFOSC	gm4+5	21,20	1500+1500	3360–9810	BD+284211
07/10/04	53286.36	+7.1	CAHA2.2m+CAFOS	B+R200	12,11	1800+1800	3180–10240	Feige110
11/10/04	53290.35	+11.1	CAHA2.2m+CAFOS	B+R200	12,11	1800+1800	3500–10280	Feige110
13/10/04	53291.79	+12.5	Lick-Shane 3-m+Kast	<i>b</i>	4.9,9.6	1500+1500	3330–10400	BD+284211,BD+174708
14/10/04	53293.40	+14.1	CAHA2.2m+CAFOS	B+R200	12,11	1800+1800	3420–10300	Feige110
21/10/04	53300.37	+21.1	NOT+ALFOSC	gm4	14.5	1200(x2)	3290–9230	BD+174708
22/10/04	53300.95	+21.7	SSO2.3m+DBS	B+R	4.8,4.8	1200+1200	3390–9200	Feige110
24/10/04	53302.95	+23.7	SSO2.3m+DBS	B+R	4.8,4.8	1200(x2)+1200(x2)	3380–9200	Feige110
30/10/04	53309.38	+30.1	NOT+ALFOSC	gm4	14.5	1200x2	3460–9230	BD+174708
15/11/04	53325.32	+46.0	CAHA2.2m+CAFOS	B200	12	2700	3380–8760	Feige110
18/11/04	53328.32	+49.0	Ekar1.82m+AFOSC	gm4	24	3600	3710–7800	–
19/11/04	53329.35	+50.1	NOT+ALFOSC	gm4	14.5	1800	3480–8910	–
23/11/04	53333.31	+54.0	CAHA2.2m+CAFOS	B+R200	12,11	2700+2700	3170–9810	Feige110
07/12/04	53347.24	+67.9	Ekar1.82m+AFOSC	gm4	24	3600	3730–7800	BD+284211
11/12/04	53351.37	+72.1	NOT+ALFOSC	gm4	19	3600	3440–8900	BD+174708
16/05/05	53506.89	+227.6	VLT-UT2+FORIS1	300V+GG375	11.5	2280+2280	3630–8900	LTT7987

Date	MJD	Phase (d)	Instrumental configuration	Grism or grating	Resolution (Å)	DITxNDITxN(ABBA) Tot. exptime (s)	Range (Å)	Standard star
02/10/04	53280.91	+2.1	TNG+NICS	AMICI prism	–	2400	7500–25000	BD+472802
22/10/04	53300.45	+21.7	AAT+IRIS2	gmJs+Hs+K	–	1440+1440+1440	10430–24800	BS7793
05/11/04	53314.84	+36.0	WHT+LIRIS	gmzJ+HK	–	2400+960	8900–23950	HD194012

^aThe phase is with respect to the *B*-band maximum (JD = 245 3279.2).

[†]Grt300/7500+Gm600/4310.

The SN lies in a region only marginally contaminated by the host-galaxy light, as well as being clear of stars in the field. Consequently, point-spread function (PSF) fitting is well suited to provide excellent estimates of the SN magnitudes. A detailed description of the photometric data reduction techniques can be found in Pastorello et al. (2007). The PSF measurements were performed using SNOOPY.³ The SN magnitudes were then measured with reference to a local sequence of 20 stars in the field of NGC 6928 (Fig. 1). These, in turn, were calibrated by comparison with photometric standard stars from the Landolt (1992) catalogue. The *U*, *B*, *V*, *R* and *I* magnitudes of the local sequence stars, obtained averaging the measurements of ~20 photometric nights, are given in Table 3.

The IR photometry was calibrated using Two-Micron All-Sky Survey (2MASS) magnitudes for a number of local standards in the field of NGC 6928, together with additional calibrations from standard fields (Hunt et al. 1998) observed on the same nights as the SN. The *K'* magnitudes of NICS and Omega2000 were converted to *K* magnitudes using the relations derived by Wainscoat & Cowie (1992).

The first steps of the spectroscopic data reduction (overscan and bias corrections, flat-fielding and trimming) are the same as for the photometry. For the IR spectroscopy, the contribution of the night sky was subtracted from the 2D IR spectrum using as reference a spectrum from a different position along the slit. Further data processing was performed using standard IRAF procedures, in particular

some tasks from the package CTIOSLIT. After the optimised extraction performed with the task APALL, the 1D spectra were wavelength calibrated in comparison to spectra of arc lamps obtained during the same night and with the same instrumental configuration. In addition, the wavelength calibration was checked against bright night-sky emission lines.

The SN spectra were then flux-calibrated using response curves derived from the spectra of standard stars (Massey et al. 1988; Hamuy et al. 1994) possibly observed during the same night. The spectra of the standard stars were also used to remove telluric features. The flux calibration of the spectra was finally checked against the photometry and, in case of discrepancy, the spectral fluxes were rescaled to match the photometry. This step is particularly important for the IR spectra, where flux tables for spectroscopic standard stars are usually not available. The typical deviation from the photometric values was less than 10 per cent (but it can be up to 20 per cent in the IR spectra).

3 PHOTOMETRY

3.1 *S*-correction

Owing to the large number of different instruments used during the optical follow-up observations of SN 2004eo, it was prudent to reduce the photometry to a standard system applying a well-tested procedure called ‘*S*-correction’, a technique which has already been applied to a number of SNe Ia (see e.g. Stritzinger et al. 2002; Krisciunas et al. 2003, 2004; Pignata et al. 2004; Elias-Rosa et al. 2006; Pastorello et al. 2007; Stanishev et al. 2007).

³ SNOOPY, originally presented in Patat (1996), has been implemented in IRAF by E. Cappellaro. The package is based on DAOPHOT, but optimised for SN magnitude measurements.

Table 3. U, B, V, R, I magnitudes of the local standards in the field of NGC 6928 (see Fig. 1). The uncertainties in brackets are the rms of the individual exposures used to estimate the average magnitudes.

ID star	U	B	V	R	I
1	16.506 (0.011)	16.505 (0.007)	15.873 (0.006)	15.472 (0.007)	15.132 (0.008)
2	16.907 (0.006)	16.729 (0.016)	16.051 (0.005)	15.624 (0.005)	15.266 (0.006)
3	18.903 (0.018)	18.491 (0.008)	17.690 (0.007)	17.197 (0.008)	16.770 (0.008)
4	18.244 (0.019)	18.009 (0.008)	17.283 (0.009)	16.829 (0.008)	16.437 (0.011)
5	18.751 (0.009)	18.581 (0.007)	17.877 (0.007)	17.433 (0.010)	17.056 (0.011)
6	18.812 (0.018)	18.998 (0.016)	18.473 (0.009)	18.061 (0.011)	17.716 (0.010)
7	18.899 (0.016)	18.647 (0.010)	17.957 (0.011)	17.513 (0.012)	17.150 (0.010)
8	18.885 (0.008)	18.278 (0.016)	17.427 (0.012)	16.840 (0.010)	16.349 (0.009)
9	18.896 (0.016)	17.720 (0.010)	16.622 (0.009)	15.918 (0.010)	15.312 (0.008)
10	18.828 (0.021)	18.637 (0.007)	17.920 (0.011)	17.501 (0.013)	17.103 (0.011)
11	18.663 (0.025)	18.734 (0.017)	18.038 (0.009)	17.682 (0.015)	17.340 (0.017)
12	17.907 (0.013)	17.819 (0.012)	17.095 (0.011)	16.684 (0.012)	16.301 (0.010)
13	18.809 (0.030)	18.115 (0.011)	17.196 (0.010)	16.695 (0.011)	16.236 (0.011)
14	19.410 (0.029)	19.096 (0.012)	18.311 (0.008)	17.800 (0.014)	17.373 (0.011)
15	18.232 (0.013)	18.274 (0.006)	17.650 (0.011)	17.235 (0.014)	16.829 (0.012)
16	19.666 (0.035)	19.591 (0.020)	18.802 (0.012)	18.334 (0.014)	17.916 (0.016)
17	19.757 (0.022)	19.241 (0.016)	18.348 (0.012)	17.780 (0.013)	17.289 (0.009)
18	18.618 (0.008)	18.350 (0.007)	17.562 (0.011)	17.101 (0.011)	16.684 (0.008)
19	18.408 (0.019)	18.248 (0.009)	17.553 (0.008)	17.084 (0.009)	16.699 (0.007)
20	15.597 (0.014)	15.562 (0.007)	14.923 (0.005)	14.544 (0.005)	14.215 (0.010)

Actually, despite the large number of instrumental configurations used, the U, B, V photometry of SN 2004eo appeared to be fairly homogeneous even without S -correction. In contrast, the original R -band and, in particular, I -band light curves show large scatter owing to differences in the filter transmission curves between the various instruments, especially for data obtained with CAFOS and ALFOSC. For details of the filter transmission curves, see Pastorello et al. (2007) and Li et al. (2001).

Application of the S -correction to the R - and I -band data significantly reduced the scatter in the light curves. Only S -corrected B, V, R and I light curves are considered in our analysis. However, for the U and IR J, H and K bands, S -corrections were not feasible because of the incomplete spectroscopic wavelength coverage and/or sparse temporal sampling. The original optical magnitudes of SN 2004eo are listed in Table 4, while the S -corrections applied to the B, V, R and I magnitudes of Table 4 are given in Table 5.

3.2 K -correction

The redshift of the host galaxy of SN 2004eo, $z = 0.016$, is sufficiently large to produce a significant effect on the observed magnitudes. In order to compare the intrinsic luminosities and colours of different SNe Ia, it is necessary to correct the photometry to the rest frame. This can be done comparing the fluxes of unredshifted and redshifted spectra of the same event through standard spectral bandpasses. In the literature, this technique is usually referred to as ‘ K -correction’, and detailed descriptions of the application to SNe Ia can be found in Leibundgut (1990), Hamuy et al. (1993), Kim, Goobar & Perlmutter (1996) and Nugent, Kim & Perlmutter (2002).

Following the prescription of Hamuy et al. (1993), and using the spectra of SN 2004eo presented in Section 4, we computed the K -correction to be applied to the photometric data of SN 2004eo. In order to cover the epochs for which no spectra were available, the corrections were linearly interpolated.

The K -corrections to be added to the $UBVRI$ SN magnitudes of Table 4 are reported in Table 6. They are typically below ~ 0.1 mag and are, in general, larger at late phases. Since the nebular spectra

evolve very slowly, the K -correction was assumed to be constant at phases later than 200 d. The S - and K -corrected optical magnitudes are reported in Table 7.

Due to the lack of adequate spectral coverage in the IR region, no K -correction was applied to the J, H and K photometry (Table 8).

3.3 Optical and Infrared Light Curves

Early-time (up to ~ 3 months post-explosion) S - and K -corrected optical light curves of SN 2004eo are shown in Fig. 2 (left-hand panel). Phase 0 corresponds to the epoch of maximum in the B -band light curve, which was estimated to have occurred on 30.7 September (JD = 245 3279.2; see Section 3.5).

Our early-time photometric coverage adequately samples all the phases of the early light curve [i.e. pre-maximum rise, B -band maximum phase, $\Delta m_{15}(B)$ decline, I -band secondary peak]. In addition, some photometry was obtained during the nebular phase. In Fig. 2 (right-hand panel), the complete U through K light curves are shown, including some additional data from the literature (Arbour et al. 2004; Gonzalez et al. 2004). Unfortunately, the U band and IR observations only commenced near maximum light, and so the coverage for these wavelengths is incomplete.

As is characteristic of SNe Ia, the V - and R -band peaks are delayed with respect to the B -band maximum, while the I -band maximum occurs a few days earlier (Section 3.5). A clear secondary peak is visible in the I -band light curve, though less prominent than usual (see Fig. 2, left-hand panel). A hint of a plateau-like feature is detectable in the R -band curve at the time of the I -band secondary maximum.

The evolution of the J -band light curve is similar to that of the I band, although the post-maximum decline is steeper ($\Delta J \approx 1.1$ mag to the minimum). At about 4 weeks, the J -band light curve shows evidence of a secondary maximum analogous to that observed in the I band. After that, the J -band light curve declines very rapidly, fading by about 1.5 mag in 3 weeks. Elias et al. (1981), Meikle (2000) and Phillips et al. (2003) noted that the H - and K -band light

Table 4. Original optical photometry of SN 2004eo.

Date	JD-240 0000	<i>U</i>	<i>B</i>	<i>V</i>	<i>R</i>	<i>I</i>	Instrument
19/09/04	53268.07			16.751 (0.010)	16.484 (0.013)		0
20/09/04	53268.76		16.689 (0.021)	16.485 (0.023)	16.238 (0.033)	16.226 (0.037)	1
21/09/04	53269.68		16.447 (0.012)	16.282 (0.010)	16.025 (0.013)	16.034 (0.013)	1
21/09/04	53270.33		16.309 (0.016)	16.133 (0.015)	15.978 (0.012)	15.833 (0.024)	2
22/09/04	53270.52		16.286 (0.014)	16.141 (0.010)	15.902 (0.014)	15.839 (0.010)	2
22/09/04	53270.67		16.188 (0.042)	16.050 (0.016)	15.807 (0.016)	15.825 (0.020)	1
23/09/04	53271.69		16.029 (0.014)	15.897 (0.012)	15.621 (0.014)	15.676 (0.016)	1
23/09/04	53272.36		15.966 (0.013)	15.858 (0.009)	15.556 (0.013)	15.549 (0.011)	2
25/09/04	53273.66		15.759 (0.016)	15.625 (0.018)	15.392 (0.018)	15.465 (0.031)	1
26/09/04	53274.69		15.662 (0.018)	15.532 (0.016)	15.272 (0.019)	15.384 (0.032)	1
26/09/04	53275.37		15.616 (0.012)	15.552 (0.011)	15.301 (0.014)	15.402 (0.011)	2
27/09/04	53275.70		15.597 (0.019)	15.451 (0.012)	15.237 (0.015)	15.398 (0.017)	1
27/09/04	53276.33		15.588 (0.013)	15.476 (0.010)	15.264 (0.013)	15.403 (0.010)	2
28/09/04	53276.70		15.536 (0.024)	15.426 (0.014)	15.179 (0.014)	15.383 (0.019)	1
28/09/04	53277.37		15.514 (0.015)	15.445 (0.009)	15.198 (0.017)	15.424 (0.009)	2
29/09/04	53277.70		15.519 (0.015)	15.370 (0.015)	15.185 (0.010)	15.398 (0.017)	1
29/09/04	53278.36		15.534 (0.012)	15.453 (0.010)	15.193 (0.012)	15.430 (0.010)	2
30/09/04	53278.71		15.504 (0.017)	15.351 (0.020)	15.160 (0.013)	15.426 (0.012)	1
01/10/04	53279.66		15.506 (0.021)	15.339 (0.014)	15.167 (0.014)	15.473 (0.015)	1
02/10/04	53280.69		15.545 (0.015)	15.329 (0.014)	15.147 (0.025)	15.492 (0.020)	1
02/10/04	53281.37			15.387 (0.010)			3
02/10/04	53281.38	15.425 (0.018)		15.385 (0.008)	15.217 (0.010)	15.613 (0.009)	3
02/10/04	53281.39	15.439 (0.018)	15.569 (0.010)	15.391 (0.009)	15.205 (0.012)	15.617 (0.012)	3
03/10/04	53281.63		15.594 (0.018)	15.338 (0.012)	15.171 (0.016)	15.534 (0.021)	1
03/10/04	53282.43		15.624 (0.011)	15.358 (0.013)	15.145 (0.013)	15.587 (0.009)	2
04/10/04	53282.68		15.634 (0.055)	15.337 (0.012)	15.160 (0.015)	15.527 (0.011)	1
04/10/04	53282.98		15.663 (0.019)	15.404 (0.013)	15.222 (0.015)	15.509 (0.035)	4
05/10/04	53283.66		15.712 (0.011)	15.386 (0.009)	15.204 (0.011)	15.569 (0.016)	1
05/10/04	53283.94		15.721 (0.011)	15.421 (0.009)	15.273 (0.011)	15.565 (0.011)	4
05/10/04	53284.36		15.780 (0.018)		15.224 (0.013)	15.626 (0.018)	2
05/10/04	53284.39		15.777 (0.011)	15.434 (0.009)	15.211 (0.010)	15.653 (0.009)	2
06/10/04	53285.33		15.895 (0.011)	15.473 (0.010)	15.267 (0.013)	15.722 (0.012)	2
06/10/04	53285.34			15.512 (0.130)			5 ^a
07/10/04	53286.30	15.946 (0.018)	15.925 (0.011)	15.490 (0.009)	15.420 (0.014)	15.570 (0.013)	6
10/10/04	53288.63		16.182 (0.013)	15.577 (0.013)	15.459 (0.020)	15.766 (0.035)	1
10/10/04	53288.92		16.243 (0.016)	15.675 (0.009)		15.777 (0.012)	4
11/10/04	53290.30	16.492 (0.018)	16.492 (0.016)	15.726 (0.047)	15.677 (0.038)	15.648 (0.022)	6
12/10/04	53290.63		16.446 (0.012)	15.747 (0.013)	15.611 (0.012)	15.825 (0.011)	1
12/10/04	53290.92		16.509 (0.011)	15.804 (0.011)		15.811 (0.011)	4
14/10/04	53292.63		16.738 (0.015)	15.902 (0.013)	15.702 (0.011)	15.817 (0.016)	1
14/10/04	53293.42	17.282 (0.019)	16.906 (0.016)	15.959 (0.011)	15.832 (0.022)	15.683 (0.013)	6
15/10/04	53294.42		16.962 (0.011)	16.036 (0.013)	15.665 (0.011)	15.919 (0.011)	2
16/10/04	53294.62		16.961 (0.027)	16.057 (0.014)	15.782 (0.015)	15.766 (0.015)	1
20/10/04	53298.61	18.125 (0.074)	17.488 (0.029)	16.334 (0.014)	15.826 (0.017)	15.768 (0.016)	7
21/10/04	53299.63		17.563 (0.235)				1
21/10/04	53300.32	18.092 (0.021)	17.529 (0.011)	16.406 (0.011)	15.984 (0.013)	15.853 (0.011)	3
22/10/04	53300.90			16.525 (0.008)			0
22/10/04	53300.92	18.165 (0.068)	17.681 (0.014)	16.530 (0.009)	16.040 (0.011)	15.827 (0.016)	0
22/10/04	53301.37		17.710 (0.041)	16.511 (0.024)	15.936 (0.012)	15.907 (0.015)	2
23/10/04	53301.60		17.681 (0.070)	16.522 (0.022)	16.031 (0.031)	15.785 (0.035)	1
24/10/04	53302.90		17.869 (0.031)	16.654 (0.025)	16.102 (0.067)	15.782 (0.088)	0
25/10/04	53303.64		17.912 (0.066)	16.675 (0.022)	16.090 (0.016)	15.766 (0.026)	1
25/10/04	53303.96		17.917 (0.041)	16.689 (0.022)	16.176 (0.015)	15.846 (0.013)	4
28/10/04	53306.92		18.159 (0.072)				4
28/10/04	53306.94		18.145 (0.059)	16.918 (0.018)	16.392 (0.021)	16.001 (0.013)	4
29/10/04	53307.93		18.224 (0.096)	16.973 (0.024)	16.447 (0.031)	16.042 (0.018)	4
29/10/04	53307.95		18.240 (0.105)				4
30/10/04	53308.61		18.200 (0.032)	16.977 (0.018)	16.415 (0.016)	16.092 (0.017)	1
30/10/04	53309.33	18.623 (0.023)	18.308 (0.011)	17.012 (0.009)	16.548 (0.010)	16.228 (0.011)	3
31/10/04	53309.90			17.091 (0.050)			4
31/10/04	53309.91			17.104 (0.017)	16.616 (0.026)		4
01/11/04	53310.60		18.218 (0.023)	17.127 (0.017)	16.601 (0.019)	16.207 (0.030)	1

Table 4 – continued

Date	JD-2400000	<i>U</i>	<i>B</i>	<i>V</i>	<i>R</i>	<i>I</i>	Instrument
02/11/04	53311.59		18.328 (0.110)	17.115 (0.060)	16.694 (0.044)	16.259 (0.115)	7
03/11/04	53312.60		18.327 (0.025)	17.194 (0.047)	16.722 (0.021)	16.316 (0.034)	1
05/11/04	53314.59		18.544 (0.029)	17.256 (0.015)	16.876 (0.059)	16.507 (0.028)	7
07/11/04	53316.60		18.608 (0.060)	17.411 (0.028)	16.965 (0.026)	16.603 (0.028)	1
08/11/04	53318.33		18.649 (0.070)	17.455 (0.029)	17.024 (0.036)	16.651 (0.035)	8
11/11/04	53320.58			17.497 (0.020)	17.095 (0.021)	16.935 (0.042)	7
12/11/04	53322.36		18.729 (0.210)				2
15/11/04	53325.27		18.810 (0.050)	17.659 (0.019)	17.243 (0.016)	17.005 (0.033)	6
15/11/04	53325.32		18.813 (0.048)				2
16/11/04	53326.21			17.656 (0.029)			8
16/11/04	53326.23		18.778 (0.054)	17.676 (0.045)	17.320 (0.050)	16.972 (0.110)	8
17/11/04	53327.24		18.786 (0.240)	17.732 (0.045)	17.375 (0.017)	17.072 (0.016)	8
18/11/04	53328.32			17.738 (0.135)	17.364 (0.155)		8
19/11/04	53328.59		18.794 (0.100)	17.740 (0.050)	17.341 (0.020)	17.145 (0.036)	1
19/11/04	53329.31		18.814 (0.240)	17.766 (0.220)			8
19/11/04	53329.32			17.775 (0.105)	17.363 (0.130)	17.217 (0.130)	8
22/11/04	53331.59		18.809 (0.500)	17.826 (0.300)	17.370 (0.220)	17.263 (0.180)	1
25/11/04	53334.53	19.109 (0.260)	18.833 (0.275)				9
25/11/04	53334.59		18.812 (0.215)	17.889 (0.065)	17.505 (0.070)	17.309 (0.200)	1
25/11/04	53335.27	19.130 (0.043)	18.913 (0.017)	17.943 (0.016)	17.560 (0.013)	17.452 (0.022)	6
28/11/04	53337.59		18.944 (0.082)	17.946 (0.027)	17.666 (0.024)	17.540 (0.037)	1
30/11/04	53339.58		18.987 (0.145)	18.014 (0.031)	17.653 (0.054)	17.673 (0.130)	7
01/12/04	53340.56			18.023 (0.046)			7
06/12/04	53346.32			18.117 (0.023)	17.937 (0.014)	17.793 (0.040)	8
07/12/04	53347.24			18.184 (0.016)			8
10/12/04	53350.19			18.264 (0.057)			8
10/12/04	53350.20		19.133 (0.048)	18.272 (0.023)	18.064 (0.032)	18.014 (0.033)	8
13/12/04	53353.20		19.239 (0.080)	18.369 (0.014)	18.156 (0.017)	18.087 (0.018)	8
14/12/04	53353.59		19.238 (0.280)	18.359 (0.080)	18.161 (0.125)	18.086 (0.215)	1
04/01/05	53375.22			18.717 (0.550)			8
09/04/05	53469.89	22.181 (0.210)					9
15/04/05	53475.88			20.702 (0.025)	21.207 (0.048)	20.914 (0.135)	9
18/04/05	53478.89		20.478 (0.018)				9
12/05/05	53502.90		21.354 (0.013)				9
13/05/05	53503.91		21.662 (0.014)	21.340 (0.011)	21.730 (0.018)	21.063 (0.023)	10
14/05/05	53504.65		21.688 (0.300)	21.354 (0.460)	≥21.60	≥21.16	6
16/05/05	53506.64		21.543 (0.050)	21.335 (0.060)	22.011 (0.087)	21.448 (0.285)	6
29/06/05	53551.49		22.260 (0.100)	21.957 (0.092)	22.619 (0.135)	22.009 (0.197)	6
02/08/05	53584.52	≥24.24	22.793 (0.190)	22.368 (0.044)	23.219 (0.120)	22.518 (0.180)	11
10/08/05	53592.69		22.842 (0.093)	22.582 (0.124)	≥23.23	≥22.14	9
23/08/05	53605.53		23.337 (0.059)				10
11/09/05	53624.55		23.521 (0.045)	23.217 (0.044)	23.633 (0.080)	22.578 (0.075)	10

0 = SSO2.3m + imager, 1 = KAIT + CCD, 2 = LT, 3 = NOT+ALFOSC, 4 = SSO1-m + WFI, 5 = Nw41-cm + CCD, 6 = CAHA2.2-m + CAFOS, 7 = Ten0.81-m + CCD, 8 = Ekar1.82-m + AFOSC, 9 = ESO/MPI2.2-m + WFI, 10 = VLT-Antu + FORS1, 11 = TNG + DOLORES.

^a This V-band observation was kindly provided by M. Fiaschi, and obtained using the 0.41-m Newton/Cassegrain Telescope of the Gruppo Astrofili di Padova, Italy, equipped with a 1024 × 1024 pixel E2V CCD.

curves of SNe Ia show a secondary maximum with brightness similar to that of the early maximum, resulting in relatively flat *H* and *K* light curves during the first month. Thereafter, the IR light curves decline steeply. A few late-time IR observations were also obtained, and the SN was recovered at ~ 230 d, $J \approx 22.2$ mag and $H \approx 20.9$ mag. The SN was not detected in the *K* band at ~ 205 d to a limiting magnitude of ~ 19.3 .

In Fig. 3, the absolute IR light curves of SN 2004eo, computed using the distance to the host galaxy discussed in Section 3.4, are compared to those of the well-observed SN 2001el (Krisciunas et al. 2003). Despite different values of $\Delta m_{15}(B)$ for the two SNe (1.15 for SN 2001el and 1.46 for SN 2004eo; see Section 3.5), the *J*, *H* and *K* light curves turn out to be quite similar.

3.4 Colour evolution and *uvoir* light curve

The excellent photometric coverage of SN 2004eo allows a detailed comparison of the colour and luminosity evolution with those of other well-studied SNe Ia. The distance of NGC 6928 was computed from the recession velocity corrected for Local Group infall into the Virgo cluster ($v_{\text{vir}} = 4810$ km s⁻¹). Assuming $H_0 = 72$ km s⁻¹ Mpc⁻¹, we obtain a distance $d \approx 67$ Mpc, or $\mu = 34.12 \pm 0.10$ mag (LEDA).

The total reddening was estimated by taking into account only the Galactic contribution, $E(B - V) = 0.109$ mag (Schlegel, Finkbeiner & Davis 1998). The Cardelli, Clayton & Mathis (1989) law was used to estimate the extinction in the different bands. The SN has

Table 5. *S*-correction to be added to the data of SN 2004eo in Table 4.

Date	JD-240 0000	<i>B</i>	<i>V</i>	<i>R</i>	<i>I</i>	Instrument
19/09/04	53268.07		0.005	-0.004		0
20/09/04	53268.76	-0.015	0	0.006	-0.001	1
21/09/04	53269.68	-0.014	0	0.006	-0.002	1
21/09/04	53270.33	-0.006	-0.014	0.017	-0.035	2
22/09/04	53270.52	-0.006	-0.014	0.017	-0.036	2
22/09/04	53270.67	-0.013	0	0.006	-0.004	1
23/09/04	53271.69	-0.012	0	0.007	-0.005	1
23/09/04	53272.36	-0.007	-0.015	0.019	-0.044	2
25/09/04	53273.66	-0.011	-0.001	0.008	-0.008	1
26/09/04	53274.69	-0.011	-0.001	0.008	-0.009	1
26/09/04	53275.37	-0.007	-0.017	0.024	-0.059	2
27/09/04	53275.70	-0.010	-0.002	0.008	-0.011	1
27/09/04	53276.33	-0.006	-0.018	0.025	-0.062	2
28/09/04	53276.70	-0.010	-0.002	0.008	-0.012	1
28/09/04	53277.37	-0.006	-0.018	0.026	-0.067	2
29/09/04	53277.70	-0.009	-0.002	0.008	-0.013	1
29/09/04	53278.36	-0.005	-0.018	0.027	-0.072	2
30/09/04	53278.71	-0.008	-0.003	0.009	-0.014	1
01/10/04	53279.66	-0.008	-0.003	0.009	-0.015	1
02/10/04	53280.69	-0.007	-0.004	0.010	-0.016	1
02/10/04	53281.38	-0.001	-0.011	0.014	-0.047	3
03/10/04	53281.63	-0.007	-0.004	0.010	-0.017	1
03/10/04	53282.43	-0.002	-0.017	0.037	-0.085	2
04/10/04	53282.68	-0.006	-0.004	0.010	-0.017	1
04/10/04	53282.98	-0.012	-0.004	-0.006	-0.020	4
05/10/04	53283.66	-0.005	-0.004	0.011	-0.017	1
05/10/04	53283.94	-0.010	-0.006	-0.006	-0.019	4
05/10/04	53284.36	-0.001	-0.017	0.043	-0.094	2
06/10/04	53285.33	0	-0.017	0.045	-0.099	2
06/10/04	53285.34		-0.028			5
07/10/04	53286.30	-0.006	-0.032	0.005	0.117	6
10/10/04	53288.63	-0.001	-0.003	0.010	-0.016	1
10/10/04	53288.92	-0.002	-0.009		-0.015	4
11/10/04	53290.30	-0.008	-0.034	0.006	0.111	6
12/10/04	53290.63	0	-0.001	0.008	-0.015	1
12/10/04	53290.92	0.002	-0.009		-0.011	4
14/10/04	53292.63	-0.001	0.002	0.007	-0.013	1
14/10/04	53293.42	-0.018	-0.034	0.007	0.096	6
15/10/04	53294.42	0.002	-0.013	0.071	-0.109	2
16/10/04	53294.62	-0.004	0.007	0.005	-0.011	1
20/10/04	53298.61	-0.004	-0.001	0.003	-0.025	7
21/10/04	53299.63	-0.012				1
21/10/04	53300.32	-0.013	-0.009	0.001	-0.044	3
22/10/04	53300.91	0.009	-0.001	-0.010	0.001	0
22/10/04	53301.37	0.002	-0.005	0.086	-0.112	2
23/10/04	53301.60	-0.015	0.020	-0.001	-0.006	1
24/10/04	53302.90	0.008	0.001	-0.012	0.002	0
25/10/04	53303.64	-0.020	0.023	-0.002	-0.005	1
25/10/04	53303.96	0.007	0.002	-0.013	0.003	4
28/10/04	53306.93	0.005	0.004	-0.014	0.005	4
29/10/04	53307.93	0.004	0.005	-0.014	0.006	4
30/10/04	53308.61	-0.027	0.025	-0.004	-0.002	1
30/10/04	53309.33	-0.026	-0.008	-0.004	-0.026	3
31/10/04	53309.91		0.006	-0.015		4
01/11/04	53310.60	-0.028	0.025	-0.005	0	1
02/11/04	53311.59	-0.010	0.005	-0.003	-0.013	7
03/11/04	53312.60	-0.028	0.024	-0.005	0.001	1
05/11/04	53314.59	-0.011	0.007	-0.001	-0.011	7
07/11/04	53316.60	-0.030	0.023	-0.005	0.004	1
08/11/04	53318.33	-0.009	0.009	-0.027	0.032	8
11/11/04	53320.58		0.005	0.002	-0.006	7
12/11/04	53322.36	-0.008				2
15/11/04	53325.27	-0.074	-0.039	0.005	-0.005	6
15/11/04	53325.32	-0.006				2

Table 5 – *continued*

Date	JD-240 0000	<i>B</i>	<i>V</i>	<i>R</i>	<i>I</i>	Instrument
16/11/04	53325.61			-0.001	0.011	1
16/11/04	53326.22	-0.007	0.009	-0.020	0.037	8
17/11/04	53327.24	-0.006	0.009	-0.019	0.037	8
18/11/04	53328.32		0.008	-0.018		8
19/11/04	53328.59	-0.016	0.016	0.001	0.013	1
19/11/04	53329.32	-0.005	0.008	-0.017	0.039	8
22/11/04	53331.59	-0.012	0.014	0.002	0.014	1
25/11/04	53334.53	-0.061				9
25/11/04	53334.59	-0.007	0.013	0.004	0.015	1
25/11/04	53335.27	-0.041	-0.045	0.002	-0.036	6
28/11/04	53337.59	-0.003	0.012	0.004	0.016	1
30/11/04	53339.58	0.001	-0.018	0.015	0.001	7
01/12/04	53340.56		-0.018			7
06/12/04	53346.32		-0.003	-0.006	0.039	8
07/12/04	53347.24		-0.004			8
10/12/04	53350.20	0.002	-0.005	-0.004	0.047	8
13/12/04	53353.20	0.003	-0.006	-0.001	0.057	8
14/12/04	53353.59	0.003	-0.006	-0.001	0.059	8
04/01/05	53375.22		-0.007			8
15/04/05	53475.88		0.055	0.059	0.126	9
18/04/05	53478.89	0.198				9
12/05/05	53502.90	0.198				9
13/05/05	53503.91	-0.028	-0.110	0.007	0.037	10
14/05/05	53504.65	0.168	0.072	-0.013	0.103	6
16/05/05	53506.64	0.168	0.072	-0.013	0.103	6
29/06/05	53551.49	0.168	0.072	-0.013	0.103	6
02/08/05	53584.52	0.111	0.163	0.214	0.100	11
10/08/05	53592.69	0.198	0.055	0.059	0.126	9
23/08/05	53605.53	-0.028				10
11/09/05	53624.55	-0.028	-0.110	0.007	0.037	10

0 = SSO2.3-m + imager, 1 = KAIT + CCD, 2 = LT + RATCAM, 3 = NOT+ALFOSC, 4 = SSO1-m + WFI, 5 = Nw41-cm GAP + CCD, 6 = CAHA2.2-m + CAFOS, 7 = Ten0.81-m + CCD, 8 = Ekar1.82-m + AFOSC, 9 = ESO/MPI2.2-m + WFI, 10 = VLT-Antu + FORS1 and 11 = TNG + DOLORES.

a peripheral location in the host galaxy and narrow interstellar Na I D lines are not detected. This suggests that the light of SN 2004eo was not significantly extinguished in the host galaxy.

We compared the colour and *uvoir* light curves of SN 2004eo with those of other normal SNe Ia (SNe 1992A, 1996X, 1994D, 2002bo, 2002er and 2003du) spanning a range of different $\Delta m_{15(B)}$ values. Comparisons were also made with the more peculiar SN 1991T (Filippenko et al. 1992b; Phillips et al. 1992) and SN 1991bg (Filippenko et al. 1992a; Leibundgut et al. 1993). In Table 9, we list the Jullian date (JD) of the *B*-band maximum, distance modulus and extinction for each SN.

As can be seen, in Fig. 4 the colour curves of SN 2004eo show an evolution similar to that of normal SNe Ia, and different from those of SN 1991bg which are redder until about +3 weeks past maximum. After the initial shift to the blue, the *B* – *V* colour of SN 2004eo reddens from 0 at +5 d to 1.2 at about +1 month. Later on (at $\geq +30$ d, Fig. 4, top), the *B* – *V* curve becomes bluer again. At late times ($\geq +200$ d), the *B* – *V* colour of SN 2004eo is unusually red (~ 0.1 mag). This colour is 0.3–0.4 mag redder than in other SNe Ia at comparable phases. Some of the difference may be attributed to the fact that most of the reference SNe are not *S*-corrected. *S*-correction can be fairly large at late phases because of the presence of strong emission lines. However, other more physical reasons may account for this anomalous late-time *B* – *V* colour (see Section 4.1).

Table 6. *K*-correction to be added to the data of SN 2004eo in Table 4.

Date	JD-240 0000	<i>U</i>	<i>B</i>	<i>V</i>	<i>R</i>	<i>I</i>	Instrument
19/09/04	53268.07			0.020	0.050		0
20/09/04	53268.76		0.047	0.022	0.050	0.058	1
21/09/04	53269.68		0.043	0.023	0.050	0.057	1
21/09/04	53270.33		0.040	0.025	0.050	0.055	2
22/09/04	53270.52		0.039	0.025	0.050	0.055	2
22/09/04	53270.67		0.039	0.026	0.050	0.054	1
23/09/04	53271.69		0.034	0.028	0.050	0.052	1
23/09/04	53272.36		0.032	0.029	0.050	0.050	2
25/09/04	53273.66		0.027	0.027	0.050	0.040	1
26/09/04	53274.69		0.025	0.025	0.050	0.029	1
26/09/04	53275.37		0.023	0.023	0.050	0.021	2
27/09/04	53275.70		0.022	0.022	0.050	0.018	1
27/09/04	53276.33		0.020	0.020	0.050	0.011	2
28/09/04	53276.70		0.019	0.020	0.051	0.009	1
28/09/04	53277.37		0.018	0.020	0.054	0.008	2
29/09/04	53277.70		0.017	0.020	0.055	0.007	1
29/09/04	53278.36		0.016	0.020	0.058	0.006	2
30/09/04	53278.71		0.015	0.020	0.059	0.005	1
01/10/04	53279.66		0.014	0.020	0.063	0.004	1
02/10/04	53280.69		0.012	0.020	0.067	0.002	1
02/10/04	53281.37			0.020			3
02/10/04	53281.38	0.059		0.020	0.070	0	3
02/10/04	53281.39	0.059	0.010	0.020	0.070	0	3
03/10/04	53281.63		0.010	0.020	0.070	0.001	1
03/10/04	53282.43		0.008	0.018	0.070	0.008	2
04/10/04	53282.68		0.008	0.017	0.070	0.010	1
04/10/04	53282.98		0.007	0.017	0.070	0.012	4
05/10/04	53283.66		0.006	0.015	0.070	0.018	1
05/10/04	53283.94		0.005	0.015	0.070	0.020	4
05/10/04	53284.36		0.003		0.070	0.024	2
05/10/04	53284.39		0.003	0.014	0.070	0.024	2
06/10/04	53285.33		0.001	0.012	0.070	0.032	2
06/10/04	53285.34			0.012			5
07/10/04	53286.30	-0.118	-0.002	0.010	0.070	0.040	6
10/10/04	53288.63		-0.007	0.004	0.059	0.034	1
10/10/04	53288.92		-0.009	0.004		0.034	4
11/10/04	53290.30	-0.135	-0.020	0	0.050	0.030	6
12/10/04	53290.63		-0.022	0	0.050	0.028	1
12/10/04	53290.92		-0.024	0		0.026	4
14/10/04	53292.63		-0.020	0	0.045	0.025	1
14/10/04	53293.42	-0.100	-0.010	0	0.040	0.030	6
15/10/04	53294.42		-0.016	-0.006	0.040	0.029	2
16/10/04	53294.62		-0.017	-0.007	0.040	0.028	1
20/10/04	53298.61	-0.078	-0.040	-0.030	0.040	0.023	7
21/10/04	53299.63		-0.046				1
21/10/04	53300.32	-0.070	-0.050	-0.040	0.040	0.020	3
22/10/04	53300.90			-0.031			0
22/10/04	53300.92	-0.089	-0.041	-0.031	0.049	0.020	0
22/10/04	53301.37		-0.038	-0.032	0.052	0.018	2
23/10/04	53301.60		-0.037	-0.033	0.053	0.017	1
24/10/04	53302.90		-0.030	-0.040	0.060	0.010	0
25/10/04	53303.64		-0.031	-0.040	0.058	0.010	1
25/10/04	53303.96		-0.032	-0.040	0.057	0.010	4
28/10/04	53306.92		-0.036				4
28/10/04	53306.94		-0.036	-0.040	0.048	0.010	4
29/10/04	53307.93		-0.038	-0.040	0.045	0.010	4
29/10/04	53307.95		-0.038				4
30/10/04	53308.61		-0.039	-0.040	0.042	0.010	1
30/10/04	53309.33	-0.140	-0.040	-0.040	0.040	0.010	3
31/10/04	53309.90			-0.040			4
31/10/04	53309.91			-0.040	0.040		4
01/11/04	53310.60		-0.040	-0.040	0.040	0.014	1
02/11/04	53311.59		-0.040	-0.040	0.040	0.017	7
03/11/04	53312.60		-0.040	-0.040	0.040	0.020	1

Table 6 – *continued*

Date	JD-240 0000	<i>U</i>	<i>B</i>	<i>V</i>	<i>R</i>	<i>I</i>	Instrument
05/11/04	53314.59		−0.040	−0.040	0.040	0.026	7
07/11/04	53316.60		−0.040	−0.040	0.040	0.033	1
08/11/04	53318.33		−0.040	−0.040	0.040	0.038	8
11/11/04	53320.58			−0.040	0.040	0.045	7
12/11/04	53322.36		−0.040				2
15/11/04	53325.27		−0.040	−0.040	0.040	0.060	6
15/11/04	53325.32		−0.040				2
16/11/04	53326.21			−0.037			8
16/11/04	53326.23		−0.043	−0.037	0.047	0.053	8
17/11/04	53327.24		−0.046	−0.034	0.053	0.046	8
18/11/04	53328.32			−0.030	0.060		8
19/11/04	53328.59		−0.042	−0.027	0.055	0.036	1
19/11/04	53329.31		−0.021	−0.020			8
19/11/04	53329.32			−0.020	0.041	0.030	8
22/11/04	53331.59		−0.037	−0.026	0.04	0.053	1
25/11/04	53334.53	−0.093	−0.048				9
25/11/04	53334.59		−0.048	−0.028	0.042	0.071	1
25/11/04	53335.27		−0.047	−0.027	0.043	0.072	6
28/11/04	53337.59		−0.044	−0.024	0.046	0.075	1
30/11/04	53339.58		−0.041	−0.021	0.049	0.077	7
01/12/04	53340.56			−0.020			7
06/12/04	53346.32			−0.011	0.059	0.084	8
07/12/04	53347.24			−0.010			8
10/12/04	53350.19			−0.010			8
10/12/04	53350.20		−0.038	−0.010	0.038	0.089	8
13/12/04	53353.20		−0.040	−0.009	0.029	0.090	8
14/12/04	53353.59		−0.040	−0.008	0.029	0.090	1
04/01/05	53375.22			0.007			8
09/04/05	53469.89	N					9
15/04/05	53475.88			0.078	−0.010	0.106	9
18/04/05	53478.89		−0.070				9
12/05/05	53502.90		−0.070				9
13/05/05	53503.91		−0.070	0.100	−0.020	0.110	10
14/05/05	53504.65		−0.070	0.100	−0.020	0.110	6
16/05/05	53506.64		−0.070	0.100	−0.020	0.110	6
29/06/05	53551.49		−0.070	0.100	−0.020	0.110	6
02/08/05	53584.52	N	−0.070	0.100	−0.020	0.110	11
10/08/05	53592.69		−0.070	0.100	−0.020	0.110	9
23/08/05	53605.53		−0.070				10
11/09/05	53624.55		−0.070	0.100	−0.020	0.110	10

N = the *K*-correction in the *U* band was not computed for these two epochs.

0 = SSO2.3-m + imager, 1 = KAIT + CCD, 2 = LT + RATCAM, 3 = NOT+ALFOSC, 4 = SSO1-m + WFI, 5 = Nw41-cm GAP + CCD, 6 = CAHA2.2-m + CAFOS, 7 = Ten0.81-m + CCD, 8 = Ekar1.82-m + AFOSC, 9 = ESO/MPI2.2-m + WFI, 10 = VLT-Antu + FORS1 and 11 = TNG + DOLORES.

Instead, there is no corresponding red excess of the late-epoch *V* – *R* and *V* – *I* colour curves (see below).

The *U* – *B* colour of SN 2004eo (Fig. 4, bottom) increases from −0.3, at a few days after maximum, to 0.5 at about +20 d. During the subsequent month, it remains almost constant, *U* – *B* ≈ 0.2 mag. The *V* – *R* colour curve of SN 2004eo (Fig. 4, top) evolves from 0.3 to −0.1 mag during the period −1 week to +1 week. It then reddens from −0.1 to 0.6 mag between +10 and +20 d, before turning blueward again (*V* – *R* ≈ −0.5 in the late nebular phase). A similar evolution is observed in the *V* – *I* colour (Fig. 4, bottom).

Fig. 5 shows the pseudo-bolometric (*uvoir*) light curve of SN 2004eo, compared to those of other SNe Ia, including the peculiar SNe 1991T and 1991bg. The *uvoir* light curve was obtained by integrating the fluxes in the optical region from the *U* band to the *I* band. The *J*-, *H*- and *K*-band data were not included because most of the comparison SNe do not have well-sampled near-IR light curves.

The light curve is similar to those of typical SNe Ia, fainter than that of SN 1991T and definitely brighter than that of SN 1991bg. In particular, SN 2004eo appears to have a luminosity evolution similar to that of SN 1992A (at least up to +1 month).

Finally, using available *J*, *H* and *K* data, we estimate the IR contribution to the SN bolometric luminosity to be negligible near maximum (~2–3 per cent), increasing to over 20 per cent by about +50 d.

3.5 Main parameters of SN 2004eo from the photometry

A χ^2 test shows that the best match to the SN 2004eo light curves in all bands is given by SN 1992A (Hamuy et al. 1996a). As shown in Fig. 6, the fit is excellent in the *B* and *V* bands, while some difference is seen in the *I* band, such as in the depth of the minimum. This is

Table 7. S- and K-corrected optical photometry of SN 2004eo.

Date	JD-240 0000	<i>U</i>	<i>B</i>	<i>V</i>	<i>R</i>	<i>I</i>	Instrument
19/09/04	53268.07			16.776 (0.014)	16.530 (0.014)		0
20/09/04	53268.76		16.721 (0.024)	16.507 (0.025)	16.293 (0.034)	16.283 (0.039)	1
21/09/04	53269.68		16.476 (0.016)	16.305 (0.013)	16.081 (0.015)	16.089 (0.019)	1
21/09/04	53270.33		16.342 (0.020)	16.144 (0.018)	16.045 (0.019)	15.853 (0.033)	2
22/09/04	53270.52		16.319 (0.018)	16.152 (0.014)	15.969 (0.020)	15.858 (0.025)	2
22/09/04	53270.67		16.214 (0.043)	16.076 (0.018)	15.863 (0.017)	15.875 (0.024)	1
23/09/04	53271.69		16.051 (0.017)	15.925 (0.015)	15.678 (0.016)	15.723 (0.021)	1
23/09/04	53272.36		15.991 (0.018)	15.874 (0.012)	15.625 (0.019)	15.555 (0.025)	2
25/09/04	53273.66		15.775 (0.020)	15.651 (0.020)	15.450 (0.019)	15.497 (0.034)	1
26/09/04	53274.69		15.677 (0.021)	15.555 (0.018)	15.330 (0.020)	15.404 (0.035)	1
26/09/04	53275.37		15.632 (0.017)	15.558 (0.015)	15.375 (0.020)	15.364 (0.026)	2
27/09/04	53275.70		15.609 (0.022)	15.471 (0.015)	15.295 (0.016)	15.405 (0.021)	1
27/09/04	53276.33		15.602 (0.017)	15.478 (0.013)	15.339 (0.019)	15.352 (0.025)	2
28/09/04	53276.70		15.545 (0.026)	15.444 (0.016)	15.238 (0.015)	15.380 (0.023)	1
28/09/04	53277.37		15.526 (0.019)	15.447 (0.013)	15.278 (0.022)	15.365 (0.025)	2
29/09/04	53277.70		15.527 (0.019)	15.388 (0.017)	15.248 (0.012)	15.392 (0.021)	1
29/09/04	53278.36		15.544 (0.017)	15.454 (0.013)	15.278 (0.019)	15.364 (0.025)	2
30/09/04	53278.71		15.511 (0.020)	15.368 (0.022)	15.228 (0.015)	15.417 (0.018)	1
01/10/04	53279.66		15.512 (0.024)	15.356 (0.016)	15.239 (0.015)	15.462 (0.021)	1
02/10/04	53280.69		15.550 (0.019)	15.345 (0.016)	15.224 (0.026)	15.478 (0.024)	1
02/10/04	53281.37			15.396 (0.014)			3
02/10/04	53281.38	15.484 (0.039)		15.394 (0.013)	15.301 (0.013)	15.567 (0.024)	3
02/10/04	53281.39	15.498 (0.039)	15.578 (0.015)	15.400 (0.013)	15.289 (0.015)	15.571 (0.025)	3
03/10/04	53281.63		15.597 (0.021)	15.353 (0.015)	15.251 (0.017)	15.519 (0.025)	1
03/10/04	53282.43		15.630 (0.016)	15.359 (0.016)	15.252 (0.019)	15.510 (0.025)	2
04/10/04	53282.68		15.635 (0.056)	15.350 (0.015)	15.240 (0.016)	15.520 (0.017)	1
04/10/04	53282.98		15.657 (0.022)	15.417 (0.016)	15.286 (0.017)	15.501 (0.038)	4
05/10/04	53283.66		15.712 (0.016)	15.397 (0.012)	15.285 (0.013)	15.570 (0.021)	1
05/10/04	53283.94		15.715 (0.016)	15.431 (0.012)	15.337 (0.013)	15.566 (0.017)	4
05/10/04	53284.36		15.782 (0.021)		15.337 (0.019)	15.556 (0.029)	2
05/10/04	53284.39		15.779 (0.016)	15.433 (0.013)	15.323 (0.017)	15.583 (0.025)	2
06/10/04	53285.33		15.896 (0.016)	15.468 (0.014)	15.382 (0.019)	15.655 (0.026)	2
06/10/04	53285.34			15.496 (0.132)			5
07/10/04	53286.30	15.828 (0.039)	15.917 (0.023)	15.468 (0.014)	15.495 (0.015)	15.727 (0.039)	6
10/10/04	53288.63		16.174 (0.017)	15.578 (0.016)	15.528 (0.021)	15.784 (0.038)	1
10/10/04	53288.92		16.232 (0.020)	15.671 (0.012)		15.796 (0.018)	4
11/10/04	53290.30	16.357 (0.039)	16.464 (0.025)	15.693 (0.048)	15.733 (0.039)	15.789 (0.043)	6
12/10/04	53290.63		16.424 (0.016)	15.746 (0.016)	15.669 (0.014)	15.838 (0.017)	1
12/10/04	53290.92		16.487 (0.016)	15.795 (0.014)		15.826 (0.017)	4
14/10/04	53292.63		16.717 (0.019)	15.904 (0.016)	15.754 (0.013)	15.829 (0.021)	1
14/10/04	53293.42	17.182 (0.040)	16.878 (0.025)	15.925 (0.016)	15.874 (0.023)	15.809 (0.039)	6
15/10/04	53294.42		16.948 (0.016)	16.017 (0.016)	15.776 (0.018)	15.839 (0.026)	2
16/10/04	53294.62		16.940 (0.029)	16.056 (0.016)	15.827 (0.016)	15.783 (0.020)	1
20/10/04	53298.61	18.047 (0.082)	17.444 (0.032)	16.303 (0.018)	15.869 (0.019)	15.766 (0.022)	7
21/10/04	53299.63		17.505 (0.235)				1
21/10/04	53300.32	18.022 (0.041)	17.466 (0.016)	16.357 (0.015)	16.025 (0.016)	15.829 (0.025)	3
22/10/04	53300.90			16.493 (0.012)			0
22/10/04	53300.92	18.076 (0.076)	17.649 (0.018)	16.498 (0.012)	16.079 (0.013)	15.848 (0.021)	0
22/10/04	53301.37		17.674 (0.043)	16.474 (0.026)	16.074 (0.019)	15.813 (0.027)	2
23/10/04	53301.60		17.631 (0.071)	16.509 (0.024)	16.083 (0.032)	15.796 (0.038)	1
24/10/04	53302.90		17.847 (0.033)	16.615 (0.025)	16.151 (0.067)	15.794 (0.089)	0
25/10/04	53303.64		17.861 (0.067)	16.657 (0.024)	16.146 (0.018)	15.771 (0.029)	1
25/10/04	53303.96		17.892 (0.043)	16.651 (0.024)	16.220 (0.016)	15.859 (0.019)	4
28/10/04	53306.92		18.128 (0.073)				4
28/10/04	53306.94		18.114 (0.060)	16.882 (0.020)	16.426 (0.022)	16.016 (0.019)	4
29/10/04	53307.93		18.190 (0.097)	16.937 (0.025)	16.478 (0.032)	16.058 (0.023)	4
29/10/04	53307.95		18.202 (0.106)				4
30/10/04	53308.61		18.134 (0.034)	16.962 (0.020)	16.453 (0.017)	16.100 (0.022)	1
30/10/04	53309.33	18.483 (0.042)	18.242 (0.016)	16.964 (0.013)	16.584 (0.013)	16.212 (0.025)	3
31/10/04	53309.90			17.057 (0.051)			4
31/10/04	53309.91			17.070 (0.019)	16.642 (0.027)		4
01/11/04	53310.60		18.150 (0.026)	17.112 (0.019)	16.636 (0.020)	16.221 (0.033)	1
02/11/04	53311.59		18.278 (0.111)	17.080 (0.061)	16.731 (0.045)	16.263 (0.116)	7

Table 7 – *continued*

Date	JD-240 0000	<i>U</i>	<i>B</i>	<i>V</i>	<i>R</i>	<i>I</i>	Instrument
03/11/04	53312.60		18.259 (0.027)	17.178 (0.048)	16.757 (0.022)	16.337 (0.037)	1
05/11/04	53314.59		18.493 (0.032)	17.223 (0.019)	16.915 (0.060)	16.522 (0.032)	7
07/11/04	53316.60		18.538 (0.061)	17.393 (0.029)	17.001 (0.027)	16.639 (0.031)	1
08/11/04	53318.33		18.599 (0.071)	17.424 (0.031)	17.037 (0.037)	16.720 (0.038)	8
11/11/04	53320.58			17.461 (0.023)	17.137 (0.023)	16.974 (0.045)	7
12/11/04	53322.36		18.681 (0.210)				2
15/11/04	53325.27		18.696 (0.054)	17.580 (0.022)	17.288 (0.017)	17.060 (0.049)	6
15/11/04	53325.32		18.767 (0.049)				2
16/11/04	53326.21			17.628 (0.031)			8
16/11/04	53326.23		18.728 (0.055)	17.648 (0.047)	17.347 (0.050)	17.062 (0.110)	8
17/11/04	53327.24		18.734 (0.240)	17.707 (0.047)	17.409 (0.019)	17.152 (0.021)	8
18/11/04	53328.32			17.716 (0.135)	17.406 (0.155)		8
19/11/04	53328.59		18.736 (0.100)	17.729 (0.050)	17.397 (0.021)	17.194 (0.038)	1
19/11/04	53329.31		18.788 (0.240)	17.754 (0.220)			8
19/11/04	53329.32			17.763 (0.105)	17.387 (0.130)	17.286 (0.130)	8
22/11/04	53331.59		18.760 (0.500)	17.814 (0.300)	17.412 (0.220)	17.330 (0.180)	1
25/11/04	53334.53	19.016 (0.262)	18.724 (0.275)				9
25/11/04	53334.59		18.763 (0.215)	17.874 (0.065)	17.551 (0.070)	17.395 (0.200)	1
25/11/04	53335.27	19.037 (0.055)	18.825 (0.026)	17.871 (0.020)	17.605 (0.014)	17.488 (0.043)	6
28/11/04	53337.59		18.897 (0.083)	17.934 (0.028)	17.716 (0.025)	17.631 (0.039)	1
30/11/04	53339.58		18.947 (0.145)	17.975 (0.033)	17.717 (0.055)	17.751 (0.131)	7
01/12/04	53340.56			17.985 (0.047)			7
06/12/04	53346.32			18.103 (0.025)	17.990 (0.016)	17.916 (0.042)	8
07/12/04	53347.24			18.170 (0.019)			8
10/12/04	53350.19			18.249 (0.058)			8
10/12/04	53350.20		19.097 (0.049)	18.257 (0.025)	18.098 (0.033)	18.150 (0.036)	8
13/12/04	53353.20		19.201 (0.080)	18.354 (0.018)	18.184 (0.019)	18.234 (0.023)	8
14/12/04	53353.59		19.201 (0.280)	18.345 (0.080)	18.189 (0.125)	18.235 (0.215)	1
04/01/05	53375.22			18.717 (0.550)			8
09/04/05	53469.89	22.181 (0.210)					9
15/04/05	53475.88			20.835 (0.028)	21.256 (0.049)	21.146 (0.136)	9
18/04/05	53478.89		20.611 (0.021)				9
12/05/05	53502.90		21.483 (0.017)				9
13/05/05	53503.91		21.565 (0.018)	21.328 (0.014)	21.718 (0.020)	21.210 (0.027)	10
14/05/05	53504.65		21.786 (0.300)	21.524 (0.460)	≥21.57	≥21.37	6
16/05/05	53506.64		21.641 (0.054)	21.507 (0.061)	21.978 (0.087)	21.661 (0.288)	6
29/06/05	53551.49		22.358 (0.102)	22.129 (0.093)	22.586 (0.135)	22.222 (0.200)	6
02/08/05	53584.52	≥24.24	22.834 (0.190)	22.630 (0.045)	23.413 (0.120)	22.728 (0.181)	11
10/08/05	53592.69		22.970 (0.094)	22.737 (0.125)	≥23.27	≥22.37	9
23/08/05	53605.53		23.239 (0.060)				10
11/09/05	53624.55		23.423 (0.046)	23.207 (0.045)	23.620 (0.080)	22.725 (0.076)	10

0 = SSO2.3-m + imager, 1 = KAIT + CCD, 2 = LT, 3 = NOT+ALFOSC, 4 = SSO1-m + WFI, 5 = Nw41-cm + CCD, 6 = CAHA2.2-m + CAFOS, 7 = Ten0.81-m + CCD, 8 = Ekar1.82-m + AFOSC, 9 = ESO/MPI2.2-m + WFI, 10 = VLT-Antu + FORS1 and 11 = TNG + DOLORES.

not surprising, since differences in the light curves of SNe Ia are usually more evident in this band (Suntzeff 1996).

The epoch and apparent magnitude of the *B*-band maximum ($JD = 245\,3279.2 \pm 0.5$, $B = 15.51 \pm 0.02$ mag) were estimated by fitting the observations of the first month with a fifth- or sixth-order polynomial. The epochs of the *V*- and *R*-band maxima were similarly determined and occur, respectively, at +1.6 and +0.9 d, while the *I*-band maximum is at about −3 d. Fitting the *I*-band light curve with a higher-degree spline, we found the epoch of the *I*-band secondary maximum to be at about +19 d (i.e. ∼22 d after the main *I*-band maximum).

Given the peak magnitude and adopted distance and reddening (see Section 3.4), the absolute *B*-band peak magnitude is $M_{B,\max} = -19.08 \pm 0.10$ mag. This is only marginally fainter than the average for normal SNe Ia (Gibson et al. 2000). The absolute magnitudes of the *V*-, *R*- and *I*-band maxima are, respectively, $M_{V,\max} = -19.13 \pm$

0.10, $M_{R,\max} = -19.19 \pm 0.10$ and $M_{I,\max} = -18.97 \pm 0.11$ mag (the uncertainties include fitting errors plus uncertainty in the distance).

The observed $\Delta m_{15}(B)_{\text{obs}}$ was found to be 1.45 ± 0.04 mag. In Table 10, we show the corresponding Δm_{15} values for the *V*, *R* and *I* bands, together with other light-curve parameters. The reddening-corrected (Phillips et al. 1999) $\Delta m_{15}(B)_{\text{true}} = 1.46$; because of the low reddening, the correction was negligible.

It has been established that the luminosity of SNe Ia correlates with the decline rate after maximum light; the slower the SN declines, the brighter the absolute peak magnitude (Pskovskii 1977; Phillips 1993; Hamuy et al. 1995, 1996b; Riess et al. 2005). More recently, other calibrations of the relations between absolute peak magnitudes and light-curve shape have been determined and refined using ever larger samples of well-studied SNe Ia.

The application of these relations reduced the scatter in the Hubble diagram of SNe Ia and significantly improved their effectiveness as

Table 8. IR photometry of SN 2004eo.

Date	JD-240 0000	<i>J</i>	<i>H</i>	<i>K</i>	Instrument
29/09/04	53278.29	15.695 (0.073)	15.985 (0.097)	15.681 (0.177)	A
01/10/04	53280.27	–	–	15.680 (0.191)	A
02/10/04	53281.43	15.834 (0.065)	15.991 (0.085)	15.677 (0.150)	B
03/10/04	53282.33	15.973 (0.077)	15.991 (0.098)	15.682 (0.337)	A
05/10/04	53284.31	16.185 (0.101)	16.077 (0.134)	15.685 (0.523)	A
07/10/04	53286.26	–	–	15.757 (0.322)	A
19/10/04	53298.28	≥16.29	–	–	A
20/10/04	53299.30	16.851 (0.145)	15.847 (0.119)	15.764 (0.182)	A
22/10/04	53300.88	16.802 (0.087)	15.788 (0.072)	15.674 (0.092)	C
29/10/04	53307.93	16.545 (0.062)	16.114 (0.085)	16.209 (0.177)	C
05/11/04	53315.29	17.165 (0.192)	–	–	D
05/11/04	53315.35	17.173 (0.097)	–	–	D
17/11/04	53326.93	18.313 (0.076)	17.015 (0.099)	–	C
18/11/04	53327.90	–	–	17.065 (0.161)	C
19/11/04	53329.32	18.254 (0.103)	17.050 (0.091)	17.226 (0.198)	B
16/04/05	53476.89	–	≥19.73	–	E
18/04/05	53478.87	–	≥20.53	–	E
21/04/05	53481.86	21.935 (0.102)	–	–	E
22/04/05	53483.68	≥21.04	≥20.05	≥19.32	F
15/05/05	53505.83	22.206 (0.282)	–	–	E
19/05/05	53509.64	–	–	≥19.05	F
21/05/05	53511.83	–	20.898 (0.312)	–	E

A = CI + SWIRCAM, B = TNG + NICS, C = AAT + IRIS2,

D = WHT + LIRIS, E = VLT-Antu + ISAAC and F = CAHA3.5-m + OMEGA2000.

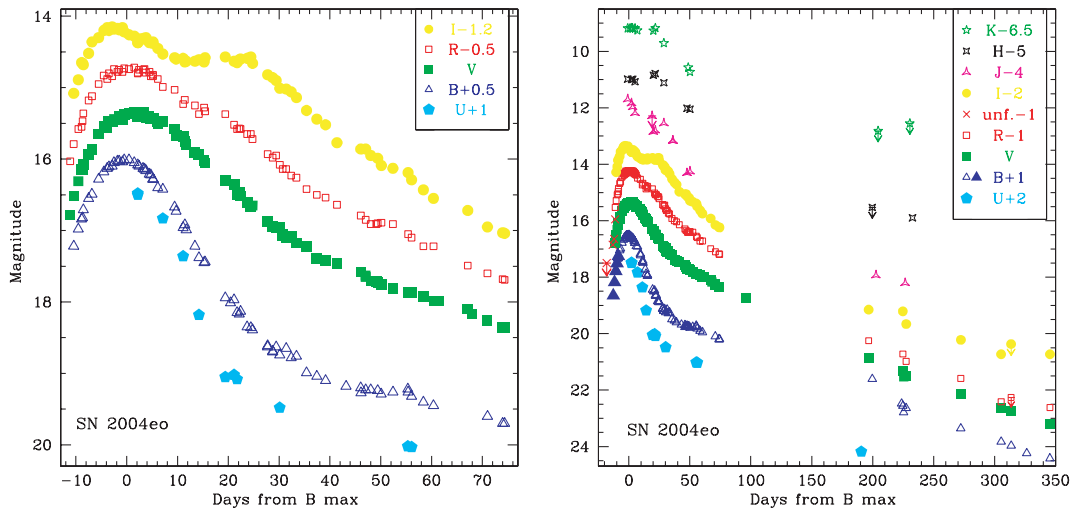


Figure 2. Left-hand panel: early-time (~ 3 months) *UBVR* light curves of SN 2004eo. Right-hand panel: complete *UBVRJHK* light curves of SN 2004eo, up to almost one year past explosion. The very early unfiltered magnitudes of Itagaki (Arbour et al. 2004) (crosses) and the early *B*-band observations of Gonzalez et al. (2004) (filled triangles) are also included. A few detection limits are shown. *S*-correction (see Section 3.1) and *K*-correction (Section 3.2) have been applied to the optical light curves (for the *U*-band photometry, *K*-correction only).

distance indicators. As detailed by Pastorello et al. (2007), we make use of some of these relations to determine the peak luminosity of SN 2004eo (see Table 11). All relations have been rescaled to $H_0 = 72 \text{ km s}^{-1} \text{ Mpc}^{-1}$.

Wang et al. (2005) recently introduced a new photometric parameter, the intrinsic *B* – *V* colour at 12 d after maximum light (ΔC_{12}). Using the relations reported in their tables 1 and 2 (see also Pastorello et al. 2007), we can derive the absolute magnitudes at maximum for the *B*, *V* and *I* bands. For SN 2004eo,

$\Delta C_{12} = 0.49 \pm 0.07$ is found. The predicted magnitudes are given in Table 11.

The different methods appear to be in good agreement. Only for the *B* magnitude obtained applying the Phillips et al. (1999) relation do we see a non-negligible deviation. Averaging the absolute magnitudes, we obtain $M_{B,\text{max}} = -18.95 \pm 0.07$, $M_{V,\text{max}} = -18.94 \pm 0.04$ and $M_{I,\text{max}} = -18.72 \pm 0.01$ mag. Given the uncertainties, these values are consistent with the directly measured magnitudes (cf. Table 10), which are marginally brighter.

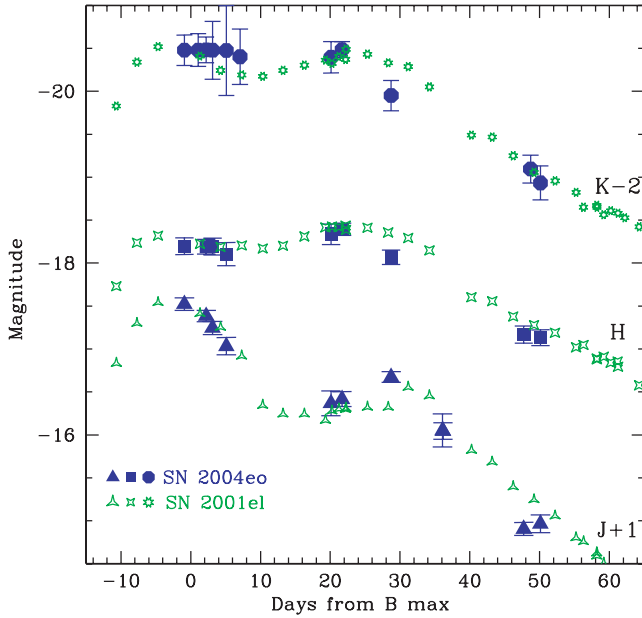


Figure 3. Comparison between the *JHK* absolute light curves of SN 2004eo and SN 2001el. Only measurement and photometric calibration errors have been taken into account for SN 2004eo. For SN 2001el, we adopted $\mu = 31.29$ mag, $E(B - V) = 0.22$ mag and a *B*-band maximum epoch of JD = 245 2182.5 (Krisciunas et al. 2003).

Table 9. Main parameters adopted for our sample of SNe Ia.

SN	JD(B_{\max})	$\Delta m_{15}(B)$	μ	$E(B - V)$	Sources
2004eo	245 3279.2	1.46	34.12	0.109	0,1
1991T	254 8374.5	0.94	30.74	0.22	2,3,4,5,6,7
1991bg	244 8605.5	1.94	31.32	0.04	5,8,9,10,11
1992A	244 8640.5	1.45	31.41 ^a	0.06	6,12,1
1994D	244 9432.5	1.31	31.14	0.03	6,11,13,14,15,16
1996X	245 0191.5	1.32	32.17	0.07	17,18,1
2002bo	245 2356.5	1.17	31.45	0.38	5,19,20,1
2002er	245 2524.16	1.33	32.87	0.36	21,1
2003du	245 2766.38	1.02	32.42	0.01	22,23,1

0 = This paper; 1 = LEDA; 2 = Schmidt et al. (1994); 3 = Lira et al. (1998); 4 = Cappellaro et al. (1997); 5 = Krisciunas et al. (2004); 6 = Altavilla et al. (2004); 7 = Saha et al. (2001); 8 = Filippenko et al. (1992a); 9 = Leibundgut et al. (1993); 10 = Turatto et al. (1996); 11 = Tonry et al. (2001); 12 = Suntzeff (1996); 13 = Richmond et al. (1995); 14 = Tsvetkov & Pavlyuk (1995); 15 = Patat et al. (1996); 16 = Meikle et al. (1996); 17 = Riess et al. (1999a); 18 = Salvo et al. (2001); 19 = Benetti et al. (2004); 20 = Stehle et al. (2005); 21 = Pignata et al. (2004); 22 = Stanishev et al. (2007); 23 = Leonard et al. (2005).

^aAverage μ from different sources.

Another useful photometric parameter is the stretch factor s^{-1} (Perlmutter et al. 1997). The measured value for SN 2004eo is $s^{-1} = 1.12 \pm 0.04$. This value is similar to that derived using a relation between s^{-1} and $\Delta m_{15}(B)_{\text{true}}$ (Altavilla et al. 2004): $s^{-1} = 1.17 \pm 0.08$.

Finally, we can estimate the explosion epoch by applying the method proposed by Riess et al. (1999b). Assuming that the SN luminosity is proportional to the square of the time elapsed since explosion and considering all photometric points starting around -8.5 d (including *B*-band measurements from Gonzalez et al. 2004), we obtain a rise time $t_r = 17.7 \pm 0.6$ d. This is a slightly short time

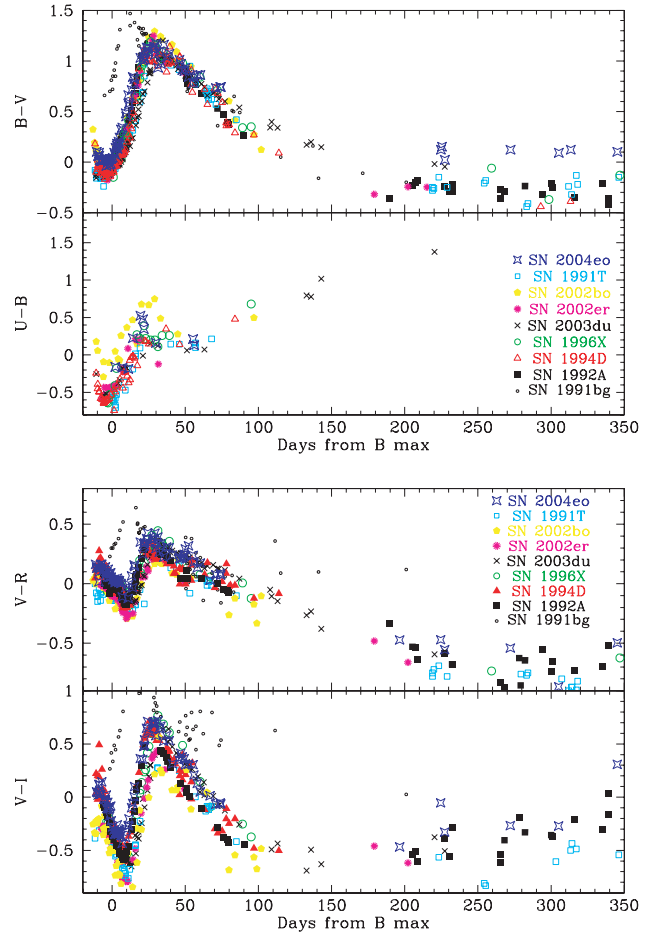


Figure 4. Colour evolution of SN 2004eo compared to other SNe Ia. Upper figure: *B - V* (top) and *U - B* (bottom) colour curves. Lower figure: *V - R* (top) and *V - I* (bottom) colour curves. *S*- and *K*-correction have been applied to the data of SN 2004eo.

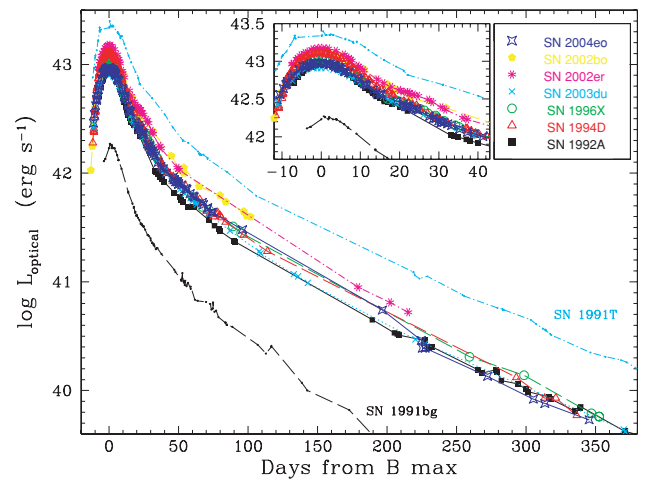


Figure 5. The integrated *UBVRi* (*uvoir*) light curve of SN 2004eo compared to those of typical SNe Ia plus the peculiar Type Ia SNe 1991T and 1991bg. The SN sample is the same as in Fig. 4. An enlarged detail of the pseudo-bolometric light curves between -12 and $+43$ d is also shown. Lacking *U*-band observations for SNe 1991bg, 1992A and 2002bo, the contribution of this band to their total luminosity was estimated following Contardo, Leibundgut & Vacca (2000).

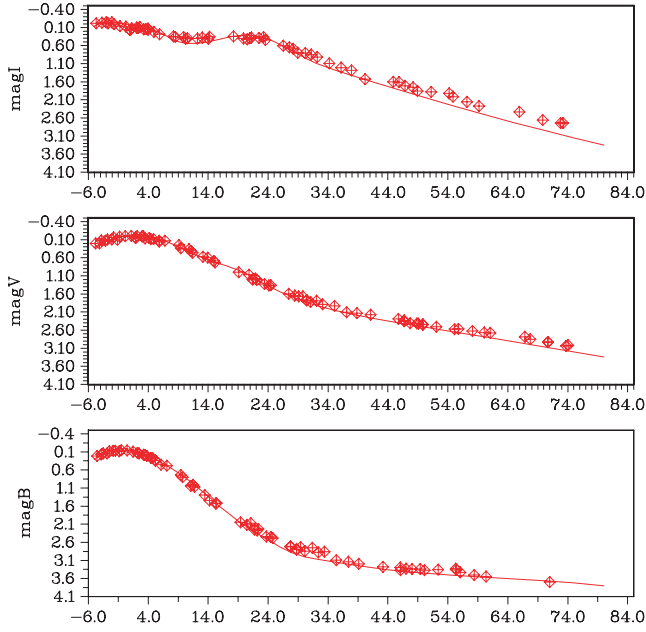


Figure 6. Comparison of the I (top), V (middle) and B (bottom) light curves of SN 2004eo with those of the template Type Ia SN 1992A (Hamuy et al. 1996a). The light curves have been offset vertically by various amounts for clarity.

for a relatively fast-declining SN Ia, but surprisingly similar to the rising time determined by Garg et al. (2007) using VR broad-band observations of a sample of 14 SNe Ia at $z = 0.11\text{--}0.35$, behind the Large Magellanic Cloud [$t_r = 17.6 \pm 1.3(\text{stat}) \pm 0.07(\text{sys})$].

Consequently, the epoch of the explosion of SN 2004eo is estimated to be $\text{JD} = 245\,3261.5 \pm 0.8$.

3.6 Ejected mass of ^{56}Ni

An important physical parameter of SNe Ia, the mass of ^{56}Ni synthesized, can be estimated by modelling the bolometric light curves. The bolometric light curve of SN 2004eo was derived from the observed *uvoir* light curve (see Section 3.4 and Fig. 5), applying the UV and IR corrections of Suntzeff (1996).

The light-curve model was computed using a grey Monte Carlo code developed by Mazzali et al. (2001). The code accounts for the propagation and deposition of gamma-ray photons and positrons emitted in the radioactive decay chain ^{56}Ni to ^{56}Co to ^{56}Fe , followed by diffusion through the ejecta of the photons which ultimately constitute the observed SN light.

In Fig. 7, we compare the bolometric light curve of SN 2004eo with the model computed for SN 2002bo (Stehle et al. 2005). This

Table 11. Decline-rate corrected absolute B , V and I magnitudes obtained by various methods (see text) and (last line) weighted averages of the different estimates. They can be compared to the absolute magnitudes derived using the distance modulus (Table 10).

Method	$M_{B,\text{max}}$	$M_{V,\text{max}}$	$M_{I,\text{max}}$
Phillips ⁽¹⁾	-18.83 ± 0.18	-18.89 ± 0.18	-18.70 ± 0.18
Altavilla ⁽²⁾	-18.99 ± 0.08		
Reindl ⁽³⁾	-18.94 ± 0.07	-18.94 ± 0.05	-18.72 ± 0.08
Wang ⁽⁴⁾	-19.01 ± 0.16	-19.00 ± 0.13	-18.72 ± 0.12
Weighted avg.	-18.95 ± 0.07	-18.94 ± 0.04	-18.72 ± 0.01

⁽¹⁾Phillips et al. (1999); ⁽²⁾Altavilla et al. (2004); ⁽³⁾Reindl et al. (2005) and ⁽⁴⁾Wang et al. (2005).

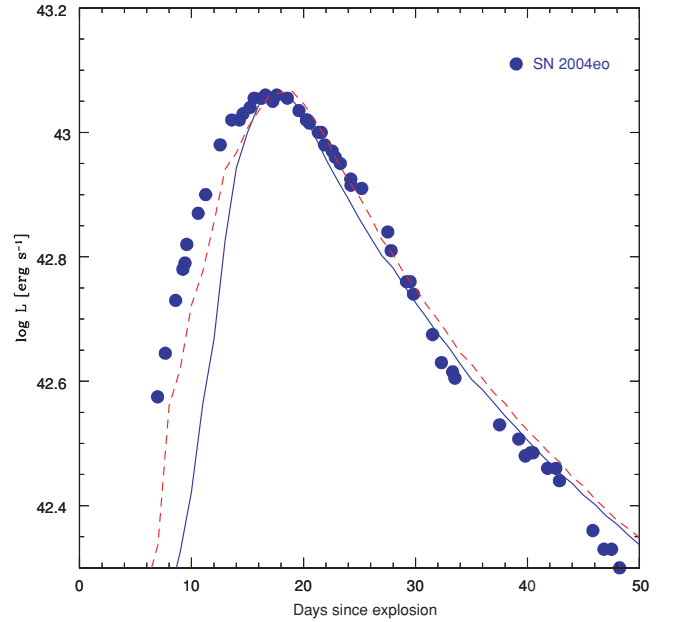


Figure 7. Comparison between the bolometric light curves of SN 2004eo (filled points), the model adopted for SN 2002bo (Stehle et al. 2005) (dashed line) and the W7-based model (solid line), both scaled to a ^{56}Ni mass of $0.45 M_{\odot}$.

originally invoked $0.50\text{--}0.55 M_{\odot}$ of ejected ^{56}Ni mass, but here it has been scaled down to $0.45 M_{\odot}$ in order to fit the lower bolometric luminosity of SN 2004eo. The bolometric light curve of SN 2004eo is slightly broader than the model, but is otherwise consistent with it. This mass is close to the lower limit of the ^{56}Ni mass range observed in normal SNe Ia, about $0.4\text{--}1.1 M_{\odot}$ (Cappellaro et al. 1997).

Table 10. Main parameters describing the $BVRI$ light curves of SN 2004eo, as derived from polynomial fits. The Galactic absorptions in the different bands are those reported by Schlegel et al. (1998). The distance modulus adopted is 34.12 mag .

Parameters	B	V	R	I
JD_{max}	$245\,3279.2 \pm 0.5$	$245\,3280.8 \pm 0.4$	$245\,3280.1 \pm 0.7$	$245\,3276.3 \pm 1.0$
$\text{JD}(\lambda)_{\text{max}} - \text{JD}(B)_{\text{max}}$	–	$+1.6^d$	$+1.0^d$	-3.2^d
A_{λ}	0.468	0.360	0.290	0.211
$m_{\lambda,\text{max}}$	15.51 ± 0.02	15.35 ± 0.02	15.22 ± 0.03	15.36 ± 0.04
$M_{\lambda,\text{max}}$	-19.08 ± 0.10	-19.13 ± 0.10	-19.19 ± 0.10	-18.97 ± 0.11
$\Delta m_{15}(\lambda)_{\text{obs}}$	1.45 ± 0.04	0.74 ± 0.04	0.57 ± 0.07	0.45 ± 0.10
$\Delta m(\text{neb}) (\text{mag}/100^d)$	1.53 ± 0.11	1.48 ± 0.06	1.60 ± 0.26	1.25 ± 0.29

For completeness, we also show in Fig. 7(a) synthetic light curve based on the W7 density distribution (Nomoto, Thielemann & Yokoi 1984) scaled to a ^{56}Ni mass of $0.45 M_{\odot}$. This yields a rather poorer reproduction of the observed light curve, especially in the rising phase. The better match of the Stehle et al. (2005) model at this time is due to their inclusion of outward mixing of ^{56}Ni .

3.7 Decline rate during the nebular phase

The *B*, *V*, *R* and *I* decline rates of SN 2004eo during the nebular phase (between +190 d and +350 d) were also computed (see Table 10, last line). The slopes of the *B*, *V* and *R* light curves (about 1.5–1.6 mag/100 d) are in good agreement with the average slope (~ 1.4 mag/100 d) computed by Lair et al. (2006) for normal and luminous SNe Ia [or HVG and LVG SNe Ia, following the nomenclature introduced by Benetti et al. (2005); see Section 5]. During this phase, the ejecta become transparent to the gamma rays and the luminosity is increasingly powered by the energy deposition of the trapped positrons. However, a fraction of the positrons may escape, resulting in a steeper light-curve decline than would be expected from the combined effects of just ^{56}Co decay and increasing gamma-ray escape. Indeed, this steeper decline in the *B*, *V* and *R* light curves is usually observed in SNe Ia at late phases (Cappellaro et al. 1997; Milne, The & Leising 1999).

The behaviour of the late-time *I*-band magnitude decline is expected to be slightly different. Lair et al. (2006) indeed found that a slower average decline rate in the late-time *I*-band light curve (0.94 mag/100 d) could be a common characteristic of normal SNe Ia. This is true also for SN 2004eo, although the *I*-band light curve actually declined at a slightly higher rate (1.25 mag/100 d). Lair et al. suggested that the reason for the slow *I*-band decline could be a shift of the late-time flux from optical to IR wavelengths. This is consistent with an almost constant IR luminosity during the nebular phase, as was found for SN 2000cx at 1–1.5 yr past the *B*-band maximum (Sollerman et al. 2004).

4 SPECTROSCOPY

Spectroscopic monitoring of SN 2004eo spanned the period -11 d to $+72$ d. Three spectra were obtained before maximum brightness, and 15 after. In addition, a late-time VLT spectrum was obtained at about eight months. IR spectroscopic observations were performed at $+2$, $+22$ and $+36$ d. Unfortunately, the resolution and/or the S/N of the IR spectra obtained for SN 2004eo are rather poor.

4.1 Optical spectra

The optical spectra of SN 2004eo obtained during the first season are shown in Fig. 8. The earliest spectra exhibit the broad P-Cygni lines typical of SNe Ia: the characteristic deep absorption near 6150 \AA due to Si II $\lambda\lambda 6347, 6371$ (hereafter Si II $\lambda 6355$), the Si II $\lambda\lambda 5958, 5979 \text{ \AA}$ feature (hereafter Si II $\lambda 5972$), the W-shaped feature near 5400 \AA attributed to S II $\lambda 5454$ and S II $\lambda 5606$. Other prominent features at pre-maximum epochs are Ca II H&K, Mg II $\lambda 4481$ and several blends due to Fe II, Si II and Si III. Fe III is also possibly detected below 5000 \AA . At red wavelengths, particularly strong features are the Ca II near-IR triplet, possibly with a high-velocity component (Mazzali et al. 2005) and Mg II $\lambda\lambda 9218, 9244$. Despite contamination from the 7600 \AA telluric feature, O I $\lambda 7774$ is clearly visible. However, there is no evidence of C II lines in the early-time spectra.

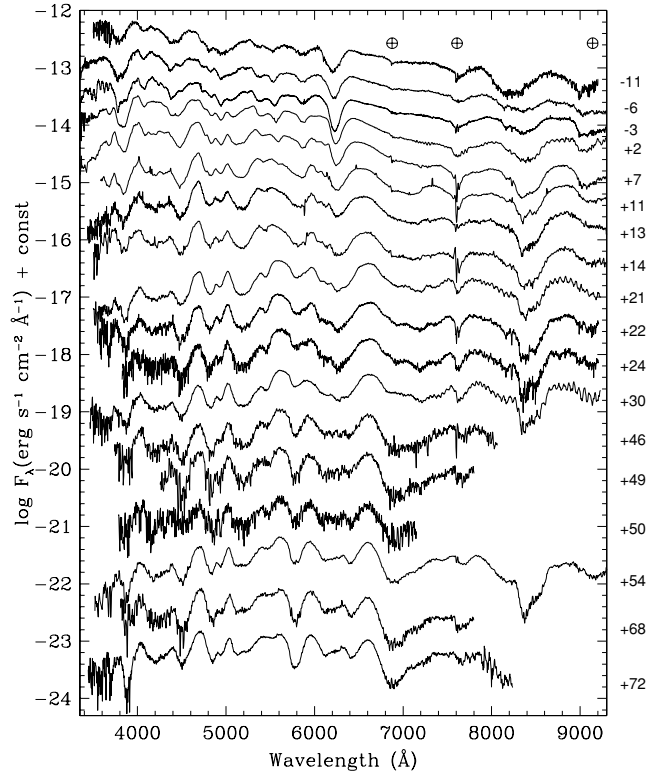


Figure 8. Evolution of the optical spectra of SN 2004eo. The spectra have not been corrected for the host-galaxy redshift. The positions of the main telluric features are marked with the symbol \oplus . The phases are labelled on the right-hand panel.

After maximum light, the Ca II near-IR triplet is very prominent, while the strengths of the Si II and S II lines rapidly decline. In particular, Si II $\lambda 5972$ is progressively replaced by the Na I D $\lambda\lambda 5890, 5896$ feature. However, Si II $\lambda 6355$ is visible up to about one month past maximum. Consistent with normal SN Ia behaviour, the post-maximum spectra show strong line blanketing at blue wavelengths due to Fe II, Ni II, Co II, Ti II and Cr II lines. Apart from the persistent Ca II H&K, Ca II near-IR triplet and Na I D features, the spectra at ~ 50 d post-maximum are dominated by iron-group lines (Branch et al. 2005).

A spectrum of SN 2004eo was obtained in the nebular phase at $+227.6$ d using the VLT UT2 equipped with FORS1 (Fig. 9). Strong forbidden lines of iron-group elements ([Fe II], [Fe III], [Ni II], [Ni III] and [Co III]) dominate the spectrum, especially in the region $4000\text{--}5500 \text{ \AA}$. Other well-developed features are also visible: Na I D, [Ca II] $\lambda\lambda 7193, 7324$ and the Ca II near-IR triplet. Moreover, the prominent feature at 4000 \AA can be tentatively identified as [S II] (Bowers et al. 1997).

As mentioned in Sections 3.4 and 3.5, there are several photometric similarities between SN 2004eo and 1992A (the shape of the light curve, the colour evolution and the quasi-bolometric luminosity). In Fig. 10 (left-hand panel), photospheric spectra of SNe 2004eo and 1992A are compared, at ~ -6 , -3 and $+7$ d. At all the epochs, the spectra of SNe 2004eo and 1992A show comparable line strengths, with some differences in the line velocities, with those of SN 2004eo being significantly lower. In Fig. 10 (right-hand panel), spectra of the same two SNe are shown, at about $+13$, $+54$ and $+227$ d. At $+227$ d, there is some difference between the two

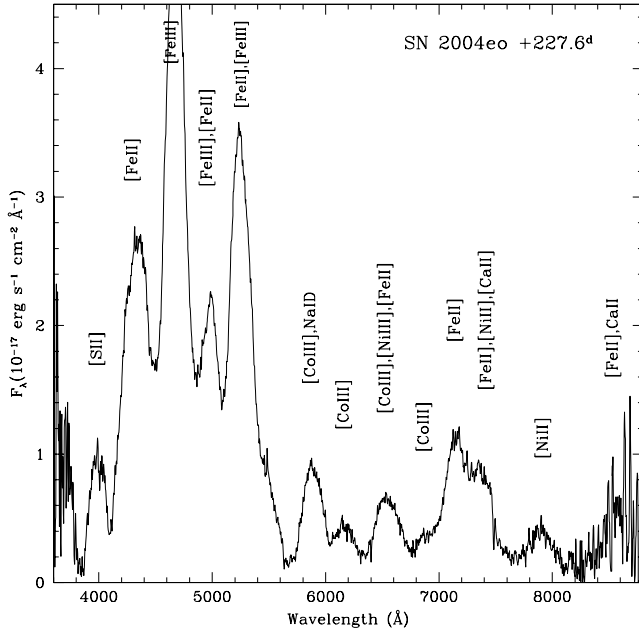


Figure 9. Nebular (phase = 227.6 d) spectrum of SN 2004eo taken with VLT + FORS1. Identifications of the main features are also shown.

events in the relative strength of features in the B and V regions, which may help to explain the anomalously red $B - V$ colour of SN 2004eo after +200 d. Below 5000 Å, the $[\text{Fe III}] \lambda 4700/[\text{Fe II}] \lambda 4300$ intensity ratio (Liu, Jeffery & Schultz 1997) appears to be lower in SN 2004eo with respect to SN 1992A. This is consistent with a slightly lower ^{56}Ni mass and hence lower temperature in SN 2004eo (Mazzali et al., in preparation). However, despite these minor differences, most of the spectral features confirm the strong similarity of the two SNe, already apparent in their photometric parameters (see e.g. Section 3.5).

In Fig. 11, pre-maximum spectra (~ -6 d, left-hand panel) and post-maximum spectra ($\sim +45$ d, right-hand panel) of SN 2004eo are compared to those of normal SNe Ia at similar phases (Benetti et al. 2004; Kotak et al. 2005; Stanishev et al. 2007; Altavilla et al., in preparation). At the pre-maximum phase of particular note is the greater prominence of the $\text{Si II } \lambda 5972$ line in SN 2004eo, again suggesting lower temperatures in this event. At +45 d, SN 2004eo shows a curious sequence of faint, narrow features in the 6000–6300 Å region. This has occasionally been observed in other SNe Ia and is probably produced by Fe II lines. An enlargement of this spectral region is shown in Fig. 12, compared to the same region of spectra of SNe 1998aq (Branch et al. 2003), 1999ac (Garavini et al. 2005) and 1999ee (Hamuy et al. 2002) at comparable phases, available in the SUSPECT⁴ archive of SN spectra.

Fig. 13 shows the same two spectra of SN 2004eo as Fig. 11, but now compared with pre-maximum (left-hand panel) and post-maximum (right-hand panel) spectra of three peculiar SNe Ia: SN 1991T (Mazzali, Danziger & Turatto 1995; Gomez & Lopez 1998), SN 2000cx (Li et al. 2001) and the underluminous (SN 1991bg-like) SN 1999by (Garnavich et al. 2004). Both the pre- and post-maximum spectra of SN 2004eo show some similarity to those of SN 1999by, although the line velocities of SN 2004eo are some-

what higher and its Si II lines (especially that at $\lambda 5972$) are slightly less prominent. But the most important difference is the lack of clear evidence, in SN 2004eo, of Ti II lines which characterize the blue spectral region of SN 1999by and other low-luminosity SNe Ia (Filippenko et al. 1992a).

4.2 Infrared spectra

Fig. 14 shows the optical and IR spectra of SN 2004eo at three epochs: +2 d, +3 weeks and about +5 weeks. The spectrum at +2 d (see Table 2) shows a blue continuum. To the red of the Ca II near-IR triplet, the Mg II doublet is visible at ~ 9230 Å (possibly blended with Mn II at 9440 Å) and the Mg II triplet at ~ 10920 Å. Moreover, a broad absorption feature near 12 100 Å may be attributed to a blend of Ca II lines. Si II dominates the broad absorption near 16 000 Å, possibly blended with Mg II lines. Despite the low-resolution, Fe II and Co II lines are also possibly detected (Marion et al. 2003). As we progress from +2 d to +22 d (see Table 2), the spectrum becomes redder. Despite the low S/N in the IR spectrum, the J band shows a prominent Fe II absorption line at ~ 12300 Å, while the H -band region is dominated by a very broad emission feature produced by iron-group lines (Fe II , Ni II , Co II). In the $\sim +30$ d spectrum (Table 2), the IR region is characterized by a number of broad, prominent features mainly due to Fe II , Ni II , Co II and Si II (Hamuy et al. 2002).

5 A BRIDGE CONNECTING DIFFERENT SUBGROUPS OF TYPE IA SUPERNOVAE?

In Section 3.5, we found that the best match to SN 2004eo is SN 1992A (Suntzeff 1996). Both these SNe show somewhat lower than normal luminosity at maximum, $M_B \approx -19.1$ mag (see Section 3.5), and rapidly declining light curves [$\Delta m_{15}(B) = 1.46$ and 1.47, respectively]. Nevertheless, there is some difference in the colours, SN 2004eo being redder than SN 1992A at late phases. There are also strong similarities in the spectroscopic evolution (Section 4.1), but again with some differences, the most significant being in the line velocities (lower in SN 2004eo) and the relative strengths of the most prominent nebular features. This mixture of similarities and differences between the two events supports the important conclusion of Benetti et al. (2004) that a single-parameter characterization of SNe Ia does not specify the full diversity of their observed behaviour (see also Hatano et al. 2000).

In spite of the fact that SN 2004eo is not particularly underluminous (see also the comparison with the bolometric light curve of the low-luminosity SN 1991bg in Fig. 5; Section 3.4), it shows some characteristics of low-luminosity SNe Ia. In general, the spectroscopic evolution, the strength of the Si II lines and the line velocities (as we will see below) are not very different from those of SN 1999by. However, while the $\Delta m_{15}(B)$ is higher and the colour redder than those of normal SNe Ia, they do not attain the extreme values of *faint* SNe Ia. These findings suggest that SN 2004eo is a normal SN Ia, but with some properties (especially the line velocities) in common with low-luminosity SNe Ia.

Benetti et al. (2005) analysed the photometric and spectroscopic properties of a sample of well-observed SNe Ia and found that they can be divided into three different subgroups:

- (i) *Faint* SNe Ia similar to SN 1991bg, showing low expansion velocities, rapid evolution of the $\text{Si II } \lambda 6355$ velocity and low peak

⁴ <http://bruford.nhn.ou.edu/~suspect/index1.html>

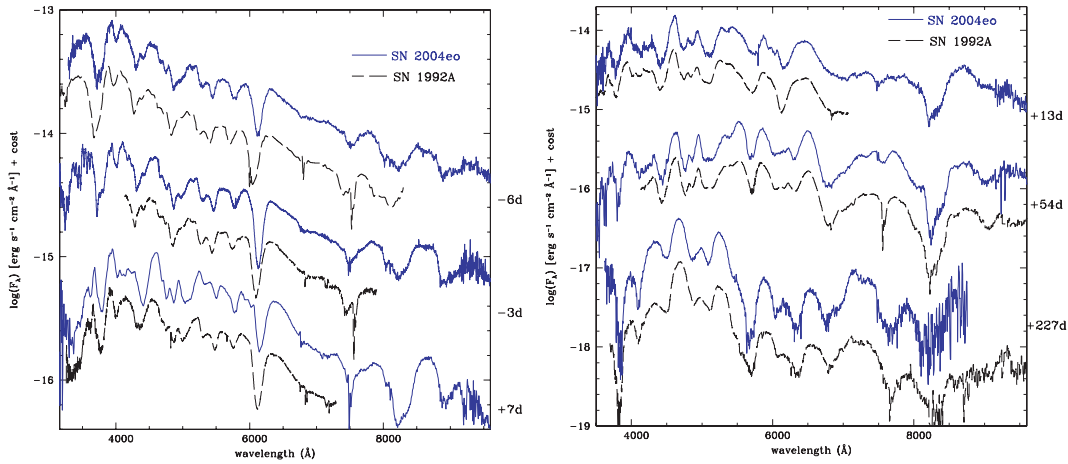


Figure 10. Left-hand panel: comparison between spectra of SN 2004eo and SN 1992A around maximum brightness. Right-hand panel: same as the left-hand panel, but for later phases. All spectra have been corrected for reddening and shifted to the host-galaxy rest frame.

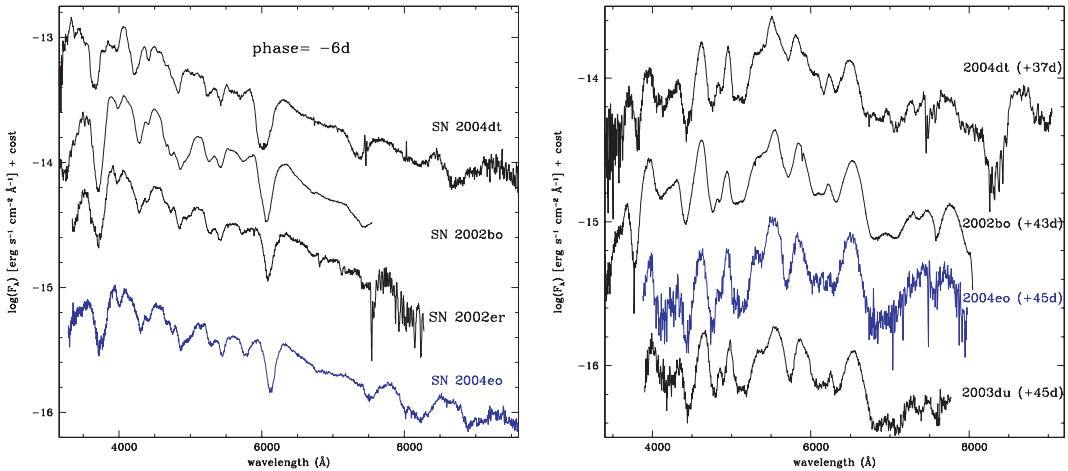


Figure 11. Left-hand panel: comparison of a pre-maximum spectrum (~ -6 d) of SN 2004eo with those of the normal SNe Ia 2004dt, 2002bo and 2002er at similar phases (acquired by the ESC). Right-hand panel: comparison of a post-maximum spectrum ($\sim +45$ d) of SN 2004eo with those of the normal SNe Ia 2004dt, 2002bo and 2003du at similar phases. All spectra have been corrected for reddening and shifted to the host-galaxy rest frame.

luminosity and temperature. The values of these parameters are the result of a low ejected ^{56}Ni mass.

(ii) Normal-luminosity (mean absolute magnitude $M_B = -19.3$ mag) SNe Ia, also showing a *HVG*, but having higher expansion velocities in the Si II lines than do the *faint* SNe Ia.

(iii) Normal and overluminous (SN 1991T-like) SNe Ia, showing a *LVG* in the Si II lines. These events populate a narrow strip in the Si II velocity evolution diagram (cf. Fig. 15).

Branch et al. (2006) have presented an alternative classification scheme in which SNe Ia are divided into four subgroups on the basis of spectroscopic properties only:

(i) *Cool* SNe Ia, whose spectra show red continua and are rich in metal lines (Ti II, Sc II, Cr II, Mg I, Ca I) that are prominent only when the temperatures are low. They correspond to the *faint* SNe Ia of Benetti et al. (2005).

(ii) *Broad-line* SNe Ia, spectroscopically normal, with relatively strong and broad Si II $\lambda 6355$. They coincide roughly with the *HVG* SNe Ia of Benetti et al.

(iii) *Core-normal* events, spectroscopically similar to the previous group, but with narrower and less prominent Si II. They form a spectroscopically highly homogeneous group and are included mainly in the *LVG* group of the Benetti et al. classification.

(iv) *Shallow-silicon* SNe Ia are spectroscopically peculiar, having a high degree of heterogeneity in observed properties. The only common feature is the weakness of the Si II absorption lines. Some examples (e.g. the high-temperature SN 1991T) show prominent Fe III features. As for the previous subdivision, they are included in the *LVG* group (Benetti et al. 2005).

However, some SNe Ia (e.g. SNe 1981B, 1989B, 1991M and 1992A; see Branch et al. 2006) are of uncertain classification. We will now compare three of these non-standard events with SN 2004eo. One of the interesting issues is whether these transition events demonstrate that there is actually a continuum of physical properties within the SN Ia class, as already established for other SN types (e.g. SNe II-P; see Hamuy & Pinto 2002; Pastorello 2003).

Benetti et al. (2005) found that, while the *faint* and *HVG* SNe Ia obey a plausible relation between $\Delta m_{15}(B)$ and the depth ratio of the

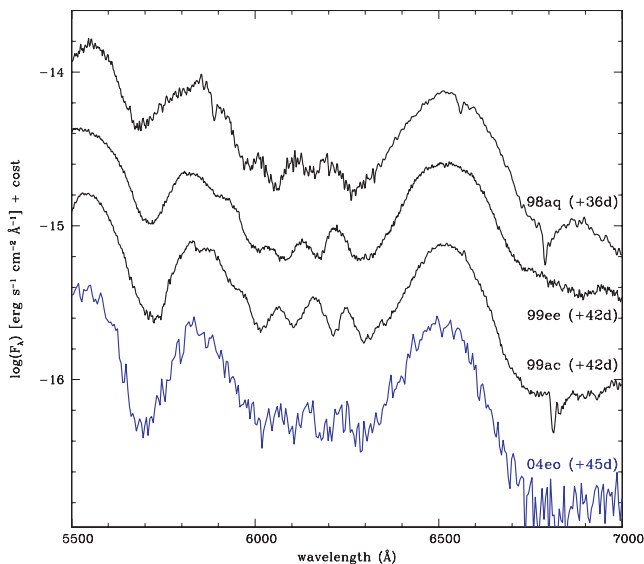


Figure 12. Detail of spectra of SN 2004eo and other SNe Ia at $\sim +40$ –45 d, illustrating the narrow, weak features in the wavelength region 6000–6300 Å.

Si II $\lambda 5972$ and Si II $\lambda 6355$ features [hereafter $R(\text{Si II})$], such a relation is weaker or even absent if the *LVG* SNe Ia are included. Also, the pre-maximum evolution of the $R(\text{Si II})$ parameter is strikingly different in *LVG* SNe Ia compared to *HVG* events.

In Fig. 15, the evolution of the velocity corresponding to the Si II $\lambda 6355$ absorption minimum is shown for SN 2004eo plus a wide range of SN Ia subtypes. The figure is an updated version of that shown by Benetti et al. (2005). The symbols are the same as those adopted by Benetti et al. The black symbols show the data for SNe 2004eo together with the non-standard events SN 1991M (Padova-Asiago Supernova Group⁵ archive), SN 1989B (Barbon et al. 1990; Wells et al. 1994) and SN 1992A (Padova-Asiago Supernova Group Archive; Kirshner et al. 1993). The latter two events were considered as *LVG* SNe Ia by Benetti et al. (2005). It is evident from Fig. 15 that SN 2004eo is a low-velocity event, lying roughly midway between the *faint* and *LVG* SNe Ia.

In Fig. 16, the time evolution of the $R(\text{Si II})$ parameter is shown for SN 2004eo and a subsample of the SNe Ia in Fig. 15. The *faint* SNe Ia, which would occupy the upper part of this diagram, are not shown. We note that for SN 2004eo, the overall evolution is similar to that of the *HVG* SNe Ia, but that it has higher $R(\text{Si II})$ values. A similar behaviour is observed for the borderline SN 1992A and (although to a lesser extent) SN 1989B (Fig. 16). These diagrams highlight the considerable heterogeneity in the observed properties of SNe Ia.

SN 2004eo plus the three non-standard events seem to follow roughly the relation between $R(\text{Si II})$ and $\Delta m_{15}(B)$ for *faint* and brighter (either *HVG* or *LVG*) events (Fig. 17, top), to some extent filling in the gap between the three subtypes. Benetti et al. (2005) found that no clear correlation exists between $dv/dt(\text{Si II})$ and $\Delta m_{15}(B)$, although the three groups of SNe Ia seem to cluster at three different positions in the diagram (Fig. 17, bottom). SN 2004eo plus the three non-standard events lie roughly in the middle of the diagram, away from any of the three clusters. In particular, the position of SN 2004eo is identical to that of SN 1992A

(as measured by Hachinger et al. 2006). As already seen in Fig. 15, these two SNe Ia seem to establish a ‘link’ between the *faint* and the *LVG* SNe Ia. SN 1989B also contributes to this bridge. In addition, SN 1991M links the *faint* and the *HVG* SNe Ia, although in this case, the lack of spectra at phases later than about +30 d makes the measurement of the velocity gradient of the Si II $\lambda 6355$ line rather uncertain and possibly overestimated.⁶

We conclude that SN 2004eo should be considered as a member of the group of non-standard or ‘transitional’ SNe Ia, along with SNe 1989B, 1991M and 1992A. These relatively rare events are characterized by a moderate-velocity gradient, relatively low ejecta velocities, peculiar $R(\text{Si II})$ evolution and moderately high $\Delta m_{15}(B)$. Branch et al. (2006) have also identified SN 1992A, SN 1989B and (possibly) the *HVG* SN 1991M (see Hachinger et al. 2006) as transitional SNe. Several other SNe Ia with $\Delta m_{15}(B)$ in the range 1.4–1.7 presented by Jha et al. (2006) and Reindl et al. (2005) are potential transitional objects (though those of Jha et al. 2006 have other peculiarities as well). This makes it possible that, as the data base of well-observed SNe Ia grows, the clustered distribution of SNe Ia in the subgroups of Benetti et al. (2005) will be less evident. Nevertheless, the majority of SNe Ia may still fall within the main subgroups.

6 CONCLUSIONS

We have presented optical and IR photometric and spectroscopic observations of the Type Ia SN 2004eo. The data range from -11 d to about +314 d from the *B*-band maximum light, with a gap of about three months when the SN went behind the Sun.

SN 2004eo has an absolute *B*-band magnitude at maximum ($M_B = -19.08$) which is close to (or only marginally fainter than) the average for SNe Ia. Consistent with its moderate luminosity, modelling of the bolometric light curve indicates that about $0.45 M_{\odot}$ of ^{56}Ni was ejected, which is close to the lower limit of the ^{56}Ni mass range observed in normal SNe Ia. However, its late-time red colour, low line velocity, high value of $\Delta m_{15}(B)$ (1.46) and evolution of the $R(\text{Si II})$ parameter are peculiar for a ‘normal’ SN Ia. Its behaviour is very similar to that of SN 1992A and (to a smaller degree) SN 1989B. These three unusual SNe Ia (together with SN 1991M) exhibit observational properties intermediate between the *faint* and more typical SNe Ia.

We conclude that there may exist a continuous range of physical properties in SNe Ia, rather than the discrete clusters proposed by Benetti et al. (2005). However, the resolution of this issue will require larger numbers of well-observed SNe Ia.

ACKNOWLEDGMENTS

This paper is based on observations collected at the 2.2- and 3.5-m telescopes of the Centro Astronómico Hispano Alemán (Calar Alto, Spain), the Asiago 1.82-m telescope and the AZT-24 Campo Imperatore Telescope (Pulkovo Observatory, Russia, and INAF Observatories, Italy), the TNG, the Liverpool telescope, the WHT and the Nordic Optical Telescope (La Palma, Spain), the ESO/MPI 2.2-m telescope (La Silla, Chile), ESO-VLT (Cerro Paranal, Chile;

⁶ The value of $dv/dt(\text{Si II})$ for SN 1991M reported by Hachinger et al. (2006) has been updated with new estimates using the spectra of Gomez, Lopez & Sanchez (1996) available in the SUSPECT archive.

⁵ <http://web.oapd.inaf.it/supern/>

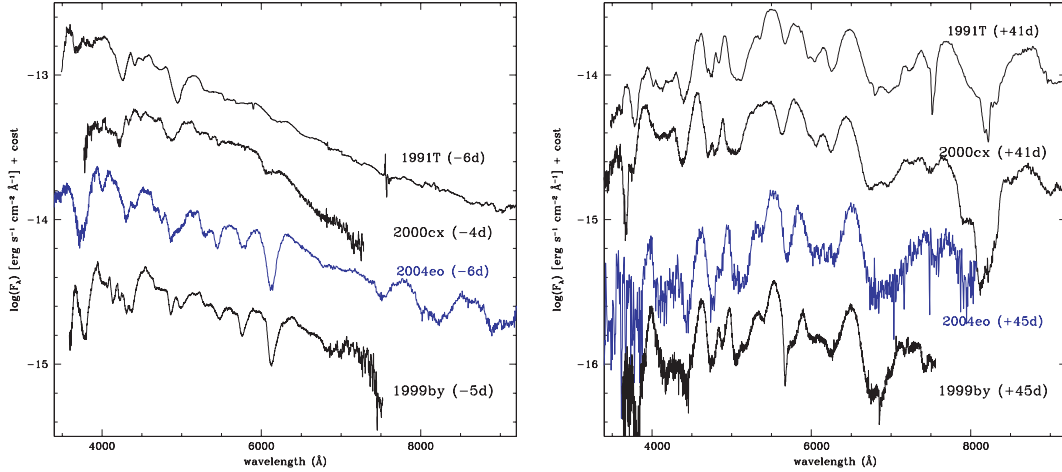


Figure 13. Left-hand panel: comparison of a pre-maximum (~ -6 d) spectrum of SN 2004eo with those of the peculiar SNe Ia 1991T, 2000cx and 1999by. Right-hand panel: as for the left-hand panel, but at $\sim +40-45$ d. All of the spectra, at both phases, have been corrected for reddening and shifted to the host-galaxy rest frame.

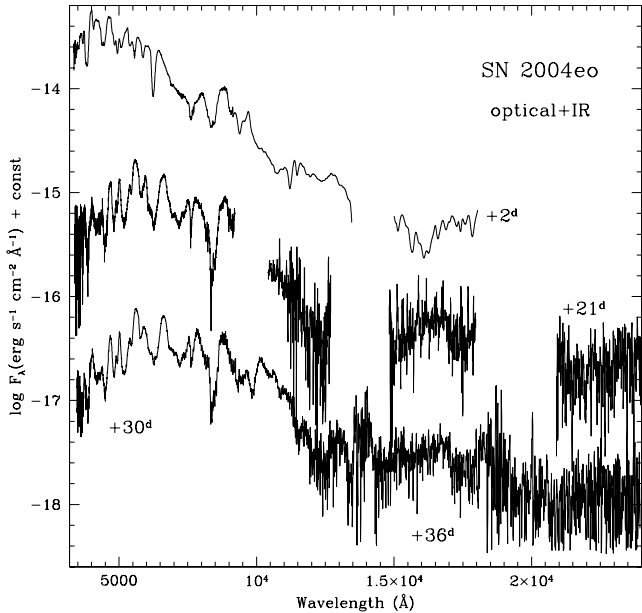


Figure 14. Optical and IR spectra of SN 2004eo at comparable epochs. The +2 d AMICI spectrum was truncated at 18 000 Å because of its poor quality. The +22 d IRIS2 spectrum was smoothed using a boxcar of 8 pixels (i.e. ~ 20 Å). No smoothing was applied to the +36 d LIRIS spectrum. This spectrum is combined with an ALFOSC optical spectrum obtained 6 d earlier.

ESO Program ID: 075.D-0346), the 0.76-m KAIT and the 3-m Shane telescope (Lick Observatory, California, USA), the AAT, the 2.3-m and 1-m telescopes (Siding Spring Observatory, Australia) and the Tenagra 0.81-m telescope (Arizona, USA). We thank the support astronomers at the Telescopio Nazionale Galileo, the Liverpool telescope, the William Herschel Telescope, the Nordic Optical Telescope, the 2.2- and 3.5-m telescopes of Calar Alto and the ESO-VLT and ESO/MPI 2.2-m telescope for performing the follow-up observations of SN 2004eo. We also thank R. Viotti for his collaboration during Target of Opportunity (ToO) observations of SN 2004eo with the Asiago 1.82-m telescope. AP thanks Marco

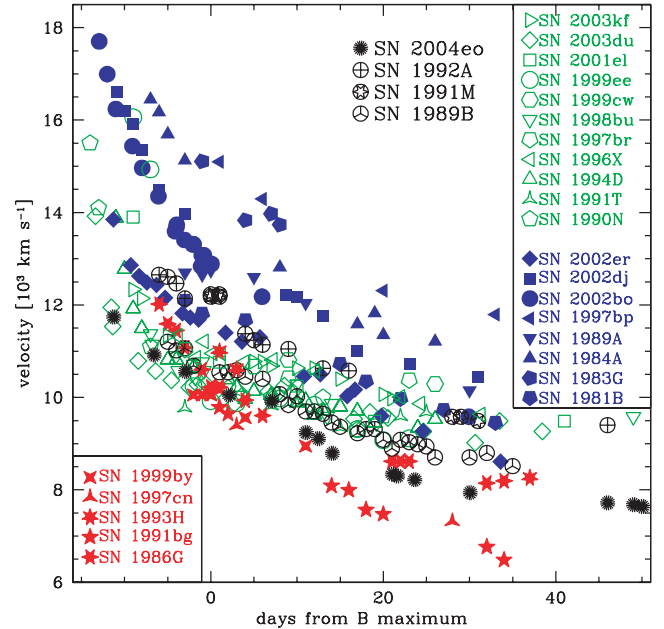


Figure 15. Evolution of the Si II $\lambda 6355$ line velocity of SN 2004eo and other SNe Ia from Benetti et al. (2005). The colours adopted for the different subclasses are the same as in Benetti et al.: starred red symbols, *faint* SNe Ia; filled blue symbols, *HVG* SNe Ia; open green symbols, *LVG* SNe Ia. The only exceptions are for SNe 2004eo together with the ‘non-standard’ SNe 1989B, 1991M and 1992A, which are labelled with black symbols (for data source references, see Benetti et al. 2005).

Fiaschi for providing a V-band observation using the 0.41-m Newton telescope of the Gruppo Astrofili di Padova.

This work was supported by the European Union’s Human Potential Programme ‘The Physics of Type Ia Supernovae’, under contract HPRN-CT-2002-00303. A.V.F.’s group at the University of California, Berkeley, is supported by National Science Foundation (NSF) grant AST-0607485 and by the TABASGO Foundation. KAIT was made possible by generous donations from Sun Microsystems, Inc., the Hewlett-Packard Company, Corporation, Lick

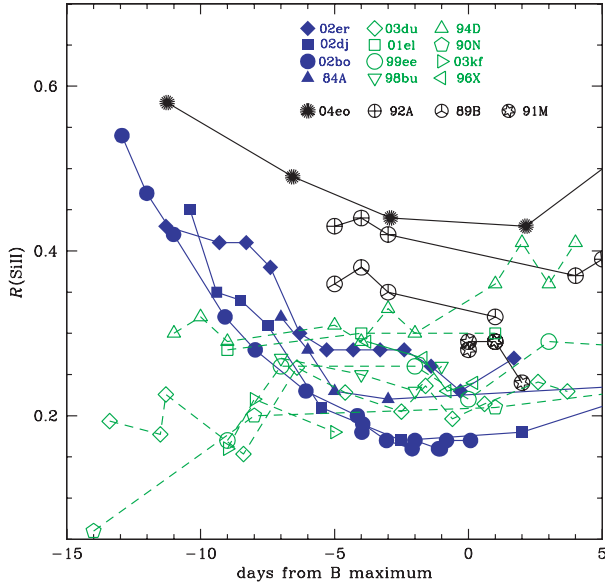


Figure 16. Evolution of the depth ratio $\text{Si II } \lambda 5972/\text{Si II } \lambda 6355$ in the spectra of SN 2004eo, together with those of other SNe Ia from Benetti et al. (2005). Green open symbols, *LVG* group; blue filled symbols, *HVG* group; black symbols, SN 2004eo plus the non-standard SNe 1989B, 1991M and 1992A.

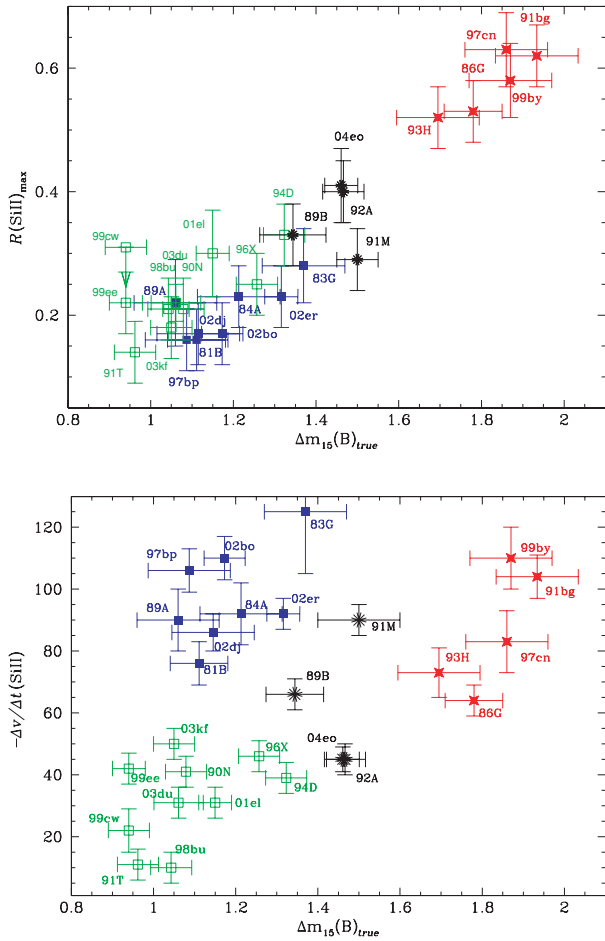


Figure 17. Top: $R(\text{Si II})_{\text{max}}$ versus $\Delta m_{15}(\text{B})_{\text{true}}$ diagram. Bottom: $dv/dt(\text{Si II})$ versus $\Delta m_{15}(\text{B})_{\text{true}}$ diagram. The non-standard events SNe 2004eo, 1989B, 1991M and 1992A are shown as black asterisks. The other SNe Ia are from Benetti et al. (2004). Red stars, *faint* SNe Ia; filled squares, *HVG* SNe Ia; open squares, *LVG* SNe Ia.

AutoScope Observatory, the NSF, the University of California and the Sylvia & Jim Katzman Foundation.

This research used the NASA/IPAC Extragalactic Data base (NED), which is operated by the Jet Propulsion Laboratory, California Institute of Technology, under contract with the National Aeronautics and Space Administration. We also made use of the Lyon-Meudon Extragalactic Data base (LEDA), supplied by the LEDA team at the Centre de Recherche Astronomique de Lyon, Observatoire de Lyon.

REFERENCES

- Altavilla G. et al., 2004, MNRAS, 349, 1344
 Arbour R., Armstrong M., Boles T., Itagaki K., Nakano S., Moore M., Li W., Briggs D., 2004, IAU Circ., 8406
 Barbon R., Benetti S., Rosino L., Cappellaro E., Turatto M., 1990, A&A, 237, 79
 Benetti S. et al., 2004, MNRAS, 348, 261
 Benetti S. et al., 2005, ApJ, 623, 1011
 Bessell M. S., 1990, PASP, 102, 1181
 Bowers E. J. C., Meikle W. P. S., Geballe T. R., Walton N. A., Pinto P. A., Dhillon V. S., Howell S. B., Harrop-Allin M. K., 1997, MNRAS, 290, 663
 Branch D. et al., 2003, AJ, 126, 1489
 Branch D., Baron E., Hall N., Melakayil M., Parrent J., 2005, PASP, 117, 545
 Branch D. et al., 2006, PASP, 118, 560
 Cappellaro E., Mazzali P. A., Benetti S., Danziger I. J., Turatto M., Della Valle M., Patat F., 1997, A&A, 328, 203
 Cardelli J. A., Clayton G. C., Mathis J. S., 1989, ApJ, 345, 245
 Contardo G., Leibundgut B., Vacca W. D., 2000, A&A, 359, 876
 Elias J. H., Frogel J. A., Hackwell J. A., Persson S. E., 1981, ApJ, 251, L13
 Elias-Rosa N. et al., 2006, MNRAS, 369, 1880
 Filippenko A. V., 2005, in Sion E. M., Vennes S., Shipman H. L., eds, *White Dwarfs: Cosmological and Galactic Probes*. Springer, Dordrecht, p. 97
 Filippenko A. V. et al., 1992a, AJ, 104, 1543
 Filippenko A. V. et al., 1992b, ApJ, 384, L15
 Filippenko A. V., Li W., Treffers R. R., Modjaz M., 2001, in Chen W. P., Lemme C., Paczyński B., eds, *Small-telescope Astronomy on Global Scales*. Astron. Soc. Pac, San Francisco, p. 121
 Garavini G. et al., 2005, AJ, 130, 2278
 Garg A. et al., 2007, AJ, 133, 403
 Garnavich P. M. et al., 2004, ApJ, 613, 1120
 Gibson B. K. et al., 2000, ApJ, 529, 723
 Gomez G., Lopez R., 1998, AJ, 115, 1096
 Gomez G., Lopez R., Sanchez F., 1996, AJ, 112, 2094
 Gonzalez S., Krzeminski W., Folatelli G., Hamuy M., Morrell N., 2004, IAU Circ., 8409
 Hachinger S., Mazzali P. A., Benetti S., 2006, MNRAS, 370, 299
 Hamuy M., Pinto P. A., 2002, ApJ, 566, L63
 Hamuy M., Phillips M. M., Wells L. A., Maza J., 1993, PASP, 105, 787
 Hamuy M., Suntzeff N. B., Heathcote S. R., Walker A. R., Gigoux P., Phillips M. M., 1994, PASP, 106, 566
 Hamuy M., Phillips M. M., Maza J., Suntzeff N. B., Schommer R. A., Aviles R., 1995, AJ, 109, 1
 Hamuy M., Phillips M. M., Suntzeff N. B., Schommer R. A., Maza J., Smith R. C., Lira P., Aviles R., 1996a, AJ, 112, 2438
 Hamuy M., Phillips M. M., Suntzeff N. B., Schommer R. A., Maza J., Aviles R., 1996b, AJ, 112, 2391
 Hamuy M. et al., 2002, AJ, 124, 417
 Hatano K., Branch D., Fisher A., Baron E., Filippenko A. V., 1999, ApJ, 525, 881
 Hatano K., Branch D., Lentz E. J., Baron E., Filippenko A. V., Garnavich P. M., 2000, ApJ, 543, L49
 Hunt L. K., Mannucci F., Test L., Migliorini S., Stanga R. M., Baffa C., Lisi F., Vanzi L., 1998, AJ, 115, 2594
 Jha S. et al., 2006, AJ, 131, 527

- Kim A., Goobar A., Perlmutter S., 1996, *PASP*, 108, 190
- Kirshner R. P. et al., 1993, *ApJ*, 415, 589
- Kotak R. et al., 2005, *A&A*, 436, 1021
- Krisciunas K. et al., 2003, *AJ*, 125, 166
- Krisciunas K. et al., 2004, *AJ*, 128, 3034
- Lair J. C., Leising M. D., Milne P. A., Williams G. G., 2006, *AJ*, 132, 2024
- Landolt A. U., 1992, *AJ*, 104, 340
- Leibundgut B., 1990, *A&A*, 229, L1
- Leibundgut B. et al., 1993, *AJ*, 105, 301
- Leonard D. C., Li W., Filippenko A. V., Foley R. J., Chornock R., 2005, *ApJ*, 632, L420
- Li W. et al., 2001, *PASP*, 113, 1178
- Lira P. et al., 1998, *AJ*, 115, 234
- Liu W., Jeffery D. J., Schultz D. R., 1997, *ApJ*, 483, L107
- Marion G. H., Höflich P., Vacca W. D., Wheeler J. C., 2003, *ApJ*, 591, 316
- Massey P., Strobel K., Barnes J. V., Anderson E., 1988, *ApJ*, 328, 315
- Mazzali P. A., Danziger I. J., Turatto M., 1995, *A&A*, 297, 509
- Mazzali P. A., Cappellaro E., Danziger I. J., Turatto M., Benetti S., 1998, *ApJ*, 499, 49
- Mazzali P. A., Nomoto K., Cappellaro E., Nakamura T., Umeda H., Iwamoto K., 2001, *ApJ*, 547, 988
- Mazzali P. A. et al., 2005, *ApJ*, 623, 37
- Meikle W. P. S., 2000, *MNRAS*, 314, 782
- Meikle W. P. S. et al., 1996, *MNRAS*, 281, 263
- Milne P. A., The L.-S., Leising M. D., 1999, *ApJS*, 124, 503
- Nomoto K., Thielemann F.-K., Yokoi K., 1984, *ApJ*, 286, 644
- Nugent P., Kim A., Perlmutter S., 2002, *PASP*, 114, 803
- Pastorello A., 2003, PhD thesis, Univ. di Padova
- Pastorello A. et al., 2007, *MNRAS*, in press (astro-ph/0702566)
- Patat F., 1996, PhD thesis, Univ. di Padova
- Patat F., Benetti S., Cappellaro E., Danziger I. J., Della Valle M., Mazzali P. A., Turatto M., 1996, *MNRAS*, 278, 111
- Perlmutter S. et al., 1997, *ApJ*, 483, 565
- Phillips M. M., 1993, *ApJ*, 413, L105
- Phillips M. M., Wells L. A., Suntzeff N. B., Hamuy M., Leibundgut B., Kirshner R. P., Foltz C. B., 1992, *AJ*, 103, 1632
- Phillips M. M., Lira P., Suntzeff N. B., Schommer R. A., Hamuy M., Maza J., 1999, *AJ*, 118, 1766
- Phillips M. M. et al., 2003, in Hillebrandt W., Leibundgut B., eds, *From Twilight to Highlight: The Physics of Supernovae*. Springer-Verlag, Berlin, p. 193
- Pignata G. et al., 2004, *MNRAS*, 355, 178
- Pskovskii Yu. P., 1977, *SvA*, 21, 675
- Reindl B., Tammann G. A., Sandage A., Saha A., 2005, *ApJ*, 624, 532
- Richmond M. W. et al., 1995, *AJ*, 109, 2121
- Riess A. G. et al., 1999a, *AJ*, 117, 707
- Riess A. G., Filippenko A. V., Li W., Schmidt B. P., 1999b, *AJ*, 118, 2668
- Riess A. G. et al., 2005, *ApJ*, 627, 579
- Saha A., Sandage A., Thim F., Labhardt L., Tammann G. A., Christensen J., Panagia N., Macchetto F. D., 2001, *ApJ*, 551, 973
- Salvo M. E., Cappellaro E., Mazzali P. A., Benetti S., Danziger I. J., Patat F., Turatto M., 2001, *MNRAS*, 321, 254
- Schlegel D. J., Finkbeiner D. P., Davis M., 1998, *ApJ*, 500, 525
- Schmidt B. P., Kirshner R. P., Leibundgut B., Wells L. A., Porter A. C., Ruiz-Lapuente P., Challis P., Filippenko A. V., 1994, *ApJ*, 434, 19
- Sollerman J. et al., 2004, *A&A*, 428, 555
- Stanishev V. et al. 2007, *A&A*, submitted
- Stehle M., Mazzali P. A., Benetti S., Hillebrandt W., 2005, *MNRAS*, 360, 1231
- Stritzinger M. et al., 2002, *AJ*, 124, 2100
- Suntzeff N. B., 1996, in McCray R., Wang Z., eds, *Supernovae and Supernova Remnants*. Cambridge Univ. Press, Cambridge, p. 41
- Taubenberger S. et al., 2006, *MNRAS*, 371, 1459
- Theureau G., Bottinelli L., Coudreau-Durand N., Gouguenheim L., Hallet N., Loulergue M., Patrel G., Teerikorpi P., 1998, *A&AS*, 130, 333
- Tonry J. L., Dressler A., Blakeslee J. P., Ajhar E. A., Fletcher A. B., Luppino G. A., Metzger M. R., Moore C. B., 2001, *ApJ*, 546, 681
- Tsvetkov D. Yu., Pavlyuk N. N., 1995, *Aston. Lett.*, 21, 606
- Turatto M., Benetti S., Cappellaro E., Danziger I. J., Della Valle M., Gouiffes C., Mazzali P. A., Patat F., 1996, *MNRAS*, 283, 1
- Wainscoat R. J., Cowie L. L., 1992, *AJ*, 103, 332
- Wang X., Wang L., Zhou X., Lou Y.-Q., Li Z., 2005, *ApJ*, 620, L87
- Wells L. A. et al., 1994, *AJ*, 108, 2233

This paper has been typeset from a $\text{\TeX}/\text{\LaTeX}$ file prepared by the author.